Chem Soc Rev

REVIEW ARTICLE

View Article Online
View Journal | View Issue

Cite this: *Chem. Soc. Rev.*, 2015, 44, 7128

Received 7th April 2015

DOI: 10.1039/c5cs00292c

www.rsc.org/chemsocrev

Zeolite membranes – a review and comparison with MOFs

N. Rangnekar,[a] N. Mittal,[a] B. Elyassi,[a] J. Caro*[b] and M. Tsapatsis*[a]

The latest developments in zeolite membranes are reviewed, with an emphasis on the synthesis techniques, including seed assembly and secondary growth methods. This review also discusses the current industrial applications of zeolite membranes, the feasibility of their use in membrane reactors and their hydrothermal stability. Finally, zeolite membranes are compared with metal–organic framework (MOF) membranes and the latest advancements in MOF and mixed matrix membranes are highlighted.

1. Introduction

Although there are several recent reviews about zeolites and MOF membranes,[1–4] some recent advances in zeolite films have not yet been reviewed. Here, we attempt to assess progress in zeolite membranes and make comparisons with MOFs.

There have been particularly significant developments in the formation of seed layers through the use of techniques such as manual assembly[5] and Langmuir trough deposition.[6] Further, secondary growth of these seed layers has advanced through novel methods such as gel-free growth[7] and minimization of twinning.[8] These and other developments have enabled the formation of sub-1 μm zeolite membranes.[9] Recent reports of 100–200 nm zeolite membranes are promising advances for their commercial viability.[10,11]

There have been some recent industrial projects that use zeolite membranes, such as for ethanol dehydration, but so far these projects have been limited. A major constraint has been the low flux and high cost, which make the required membrane area to be economically unviable.[12] With an order of magnitude reduction in zeolite membrane thickness, there are now new opportunities for industrial applications.

We also review several other important topics which have not been covered in recent zeolite membrane reviews, such as, local permeance characterization, hydrothermal stability and modeling of permeation. The main differences between zeolites and MOF membranes are highlighted, with a focus on synthesis strategies. Finally, recent work on polymer supported zeolite and MOF membranes as well as mixed matrix membranes is summarized. The high cost of the ceramic support, which was also a major factor preventing industrial application, may soon be replaced by relatively inexpensive polymer supports.

[a] *Department of Chemical Engineering and Materials Science, 421 Washington Ave SE, Minneapolis, MN 55455, USA*

[b] *Institut für Physikalische Chemie und Elektrochemie der Leibniz Universität Hannover, Callinstr. 2, D-30167 Hannover, Germany*

N. Rangnekar

Neel Rangnekar received his Bachelors in Chemical Engineering from the Institute of Chemical Technology (earlier known as UDCT), Mumbai. He is currently a PhD candidate at the University of Minnesota advised by M. Tsapatsis. His thesis topic is the synthesis and characterization of membranes for xylene separation using zeolite nanosheets.

N. Mittal

Nitish Mittal received his Bachelors and Masters in Chemical Engineering from the Indian Institute of Technology Kanpur. He is currently a PhD candidate at the University of Minnesota advised by M. Tsapatsis and P. Daoutidis and works on modeling and optimization of zeolite membrane systems.

We believe that this review comes at a critical time that major recent advances in the field of zeolite and MOF membranes should lead to new industrial applications to ensure the reliability of the field.

2. Progress in seeding techniques

Since self-supporting thin zeolite layers cannot be handled, mainly because of mechanical problems, the molecular sieve layer (zeolite, MOF *etc.*) is usually directly grown on a porous ceramic or a metal support. However, zeolite nucleation and subsequent crystal growth on the surface of such supports is difficult to control. A well-established method for the growth of thin and defect-free molecular sieve layers is based on seeding and secondary growth. Seed crystallites of the desired zeolite or the MOF are synthesized *ex situ*. In a second step these seed crystallites are brought by different techniques using electrostatic forces (zeta potential differences), covalent chemical anchoring or capillary forces during dip or spin coating to the support surface. Finally, these seed crystallites can grow *in situ* to a homogeneous thin film.

2.1. Synthesis of zeolite seeds

Traditionally, zeolite seeds have been synthesized by direct (bottom-up) synthesis strategies. For all-silica or high-silica zeolites, this typically involves hydrothermal treatment of a sol containing a silica/alumina source, an organic structure directing agent (SDA) and water. SDA-free synthesis of certain zeolites is also possible.[13] There are several reports on shape control of zeolite seeds, *i.e.* favoring growth along certain crystalline directions and suppressing growth along others.[14–16] This is usually done by changing the SDA structure or the growth conditions. There exist several studies on the influence of these conditions on zeolite nucleation and growth, which are summarized in a review article.[17]

The top-down approach for seed synthesis, in which a parent material is first synthesized and then broken down or modified in order to yield seeds, has been considerably advanced. In one approach, three-dimensionally ordered mesoporous zeolites are synthesized within carbon templates. They can be disassembled to give spherical nanoparticles precisely sized in the 10–50 nm range, which is not readily accessible by direct synthesis.[18–20] Another approach involves exfoliation of layered zeolites[21,22] and has been discussed recently in a perspective.[23] Although zeolite exfoliation was reported in 1998,[24] only recently MFI and MWW suspensions containing exfoliated nanosheets at sufficient quantity and quality for membrane application were reported.[25] It was further shown that nanosheets could be coated on alumina supports and secondary-grown to form selective membranes. For this approach, it is important to develop methods to remove large, unexfoliated particles which can

B. Elyassi

Bahman Elyassi received his BS and MS degrees from the University of Tehran and his PhD in chemical engineering from the University of Southern California. He is currently a postdoctoral associate at the University of Minnesota. His research interests include separation and purification technologies using membranes and adsorbents.

J. Caro

Juergen Caro (1951) studied chemistry and obtained PhD from Leipzig University in 1977. Since 2001 he has been the chair of Physical Chemistry at Hannover University. J. Caro is the author of about 300 publications and 38 patents. He is a visiting professor at the Chinese Academy of Sciences and at the Dalian University of Technology. He together with M. Tsapatsis in 2013 received the Breck Award of the International Zeolite Association and the Ostwald Medal of the Saxonian Academy of Sciences.

M. Tsapatsis

Michael Tsapatsis joined the Department of Chemical Engineering and Materials Science at the University of Minnesota in September 2003 as a professor and he currently holds the Amundson Chair. He received an Engineering Diploma (1988) from The University of Patras, Greece, and MS (1991) and PhD (1994) degrees from the California Institute of Technology (Caltech) working with G. R. Gavalas. He was a post-doctoral fellow with M. E. Davis at Caltech (1993–1994). Before joining the University of Minnesota he was a faculty member in the Chemical Engineering Department at the University of Massachusetts Amherst (1994–2003). He is a fellow of the American Association for the Advancement of Science and a member of the National Academy of Engineering.

compromise membrane performance.[10] The exfoliated MFI nanosheets were coated using vacuum filtration to form an 80 nm-thick seed layer, which was secondary grown to give a 200 nm-thick membrane. In a recent work, it was shown that the gel-free secondary growth method (see Section 3) can be used in combination with nanosheet seeding to obtain MFI membranes of 100–200 nm thickness which are highly selective for xylene and butane isomer separation.[11]

2.2. Techniques for seed assembly

2.2.1. Manual and self-assembly. Manual and self-assembly of seed monolayers was studied extensively by Yoon and co-workers and it has been reviewed in 2007.[26] According to one version of this technique, zeolite seeds are manually rubbed on a substrate. Either ionic bonding or hydrogen bonding was found to be responsible for the assembly. For example, ionic bonding could be induced between trimethylpropylammonium groups on silicalite-1 and butyrate groups tethered to glass. Hydrogen bonding occurs by direct bonding of hydroxyl groups on silicalite-1 crystals and those on glass or mediated by poly(ethyleneimine). A direct covalent bonding between the support and the seed crystals can be established by using water-soluble bi-dentate additives like di-isocyanates as proposed by Yoon.[27] In a first step, the OH groups of the support react with an isocyanate group and in a second step the OH groups of the seed crystals react with the other isocyanate group which results in a strong attachment of the seed crystals to the support.

Fig. 1 shows the attachment of seeds to an oxidic support surface using the bidentate di-isocyanate as a linker.[28]

Another way for the attachment of seed crystals is the treatment of the ceramic support with aminopropyl-triethoxysilane (APTES) before synthesis.[29] The ethoxy groups react with surface hydroxyl groups of the support resulting in an amino group anchored to the support with a positive zeta potential. The reversal in charge from a negative to a positive can also be obtained by van der Waals adsorption of positively charged macromolecules.[30]

In subsequent studies, this method has been used to obtain continuous a- and b-oriented MFI films by manually assembling the seeds followed by secondary growth.[5] In a recent work, a 200 nm thick b-oriented MFI membrane on porous silica support was obtained by manual assembly followed by gel-free secondary growth.[7] Fig. 2a and b show the seed layer generated by manual assembly. Fig. 2c and d show the final membrane obtained by secondary growth using gel-free secondary growth (see Section 3).

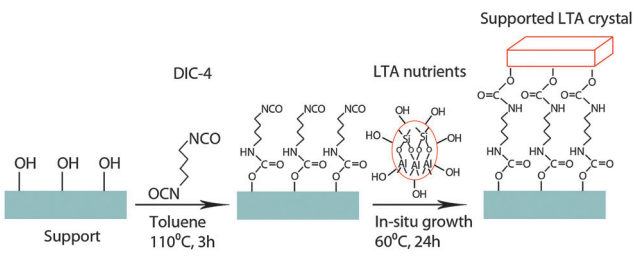

Fig. 1 Covalent attachment of seed crystals to a ceramic surface by di-isocyanate as a bidentate linker between the seed crystallite and the support. Reproduced from ref. 28 with permission from the Royal Society of Chemistry.

Other groups have also successfully adapted the Yoon technique in recent years for the synthesis of zeolite films or membranes.[31–37]

Recently, Hedlund and co-workers extended the manual assembly technique to nanocrystals by controlling the humidity of the environment during the coating process.[38] The authors proposed, as shown in Fig. 2, that for hydrophilic substrates like hydroxypropyl cellulose (HPC), at high relative humidity, assembly is mediated by hydrogen bonding with water molecules from the vapor phase (Fig. 2e). At lower humidity, the hydroxyl groups on the substrates prefer to bond with each other and nanocrystal assembly is not as strongly favored (Fig. 2g). For less hydrophilic substrates like poly(methylmethacrylate) (PMMA), high humidity causes the hydroxyl groups to be converted to epoxy groups and nano-crystal assembly is not favoured. Low humidity allows favorable contact between the crystals and the surface (Fig. 2f and h).

Manual assembly has been adapted as a facile seeding technique for lab-scale efforts. An important point to note regarding rubbing by hand is that gloves must be used due to safety considerations.

Although manual assembly is not currently scalable for large area membrane fabrication, it could be scaled up by automation of the rubbing process. Rubbing by a rotating or a lateral polishing device could be envisioned for large scale application of this technique. Moreover, sonication assisted deposition could also offer a route towards scalable implementation.[39]

2.2.2. Langmuir trough assembly. Langmuir trough deposition has been typically used in the past to obtain monolayers of surfactant molecules and other non-zeolitic materials.[40–43] A recent review summarizes the current state of the art of this technique.[44] Its use to obtain coatings of zeolites is a more recent development. Following an initial report in 2002, in which a commercial micron-sized zeolite was deposited from the air–water interface onto a silicon wafer,[45] there have been several attempts to obtain thin films of zeolite particles on substrates. In 2007, it was shown that 500 nm thick intergrown films of silicalite-1 could be obtained on silicon wafers by deposition of 95 nm seeds followed by secondary growth.[46] In the same year, monolayer films of zeolite beta of two different sizes (1 μm and 180 nm) were also obtained on silicon wafers.[47] The following year, 100 nm silicalite-1 seeds were deposited as monolayers using the Langmuir–Blodgett (LB) technique.[48] Deposition was followed by secondary growth, resulting in a ~100 nm thick intergrown zeolite film. Recently, LB was used to obtain a 1.5 μm intergrown film,[49] while an attempt was made to extend the approach to porous supports[50] with the goal of obtaining zeolite membranes.

Moreover, the Langmuir–Blodgett and Langmuir–Schaefer techniques were used to deposit 3 nm thick MFI nanosheet seeds (previously discussed) on silicon wafers.[6] This advancement allowed the formation of an ultrathin seed layer which could be

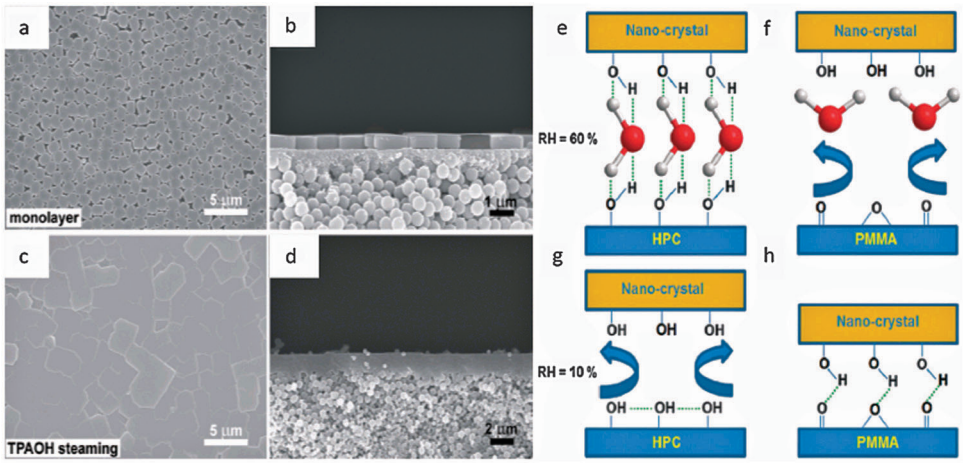

Fig. 2 (a) Top-view of rubbed MFI seeds on the silica fiber support, (b) cross-sectional view of the same seed layer, (c) top-view of MFI membrane after gel-free secondary growth, (d) cross-sectional view of the same membrane. ((a)–(d) Reproduced from ref. 7 with permission from Wiley-VCH). (e)–(h) Influence of humidity on nano-crystal assembly on two different substrates (HPC and PMMA). (e), (f) Assembly at 60% relative humidity; (g), (h) assembly at 10% relative humidity. ((e)–(h) Reproduced from ref. 38 with permission from the Royal Society of Chemistry.)

subjected to secondary growth to obtain a continuous film. The final film thickness is sub-12 nm, which is the thinnest intergrown MFI film reported.

Although intergrowth of seed layers prepared by the Langmuir–Blodgett deposition method has been demonstrated, there is no evidence for macroscopic continuity. From our experience, using LB to form coatings with uniform packing over hundreds of micrometers reproducibly can be challenging. Therefore, although continuous LB deposition can be realized we remain sceptical regarding the potential of this approach for large scale zeolite membrane manufacturing. The approach appears to be better suited to metal organic framework (MOF) films and membranes made by stepwise deposition of reactants, liquid phase epitaxy and other layer-by-layer assembly approaches.[51–58]

2.2.3. Varying temperature hot dip coating. In the recent literature, there are reports of practical significance with respect to scalable production of zeolite membranes based on a varying temperature hot dip-coating (VTHDC) method,[59,60] which is capable of making seed layers while also plugging defects on the support. In this technique, a tubular support (for example, alumina) is inserted into a solution containing large zeolite seeds at high temperature (177 °C). After removal of the superfluous crystals by rubbing, the support is dipped into a suspension containing smaller seeds at a lower temperature (77 °C) and withdrawn. This seeding method is reported to allow for reproducible membrane manufacturing of relatively thick films on coarse supports.

3. Secondary growth developments

After seeding of the support, a hydrothermal growth step is usually required in order to induce secondary growth of zeolite seeds and close gaps, which are detrimental to membrane performance. Synthesis of a selective membrane without the use of secondary growth has so far not been achieved for zeolites but it has been achieved in other materials, including graphene oxide[61] and MOFs.[62] Development of large aspect ratio nanosheets may enable selective seed layers even in the case of zeolites, by enabling good overlap of nanosheets and minimizing gaps. However, up to now, secondary growth remains a necessary, albeit undesirable step from the large scale production standpoint.

A very important development in secondary growth of zeolite membranes was achieved by Pham *et al.* recently.[7] They reported a gel-free method of secondary growth which uses a small quantity of structure directing agent but circumvents the use of a gel for growth. Instead, the silica source for secondary growth comes from the support. A precursor version of such a process was published by Chaikittisilp *et al.*,[63] who showed that the amorphous silica layer on a silicon wafer could be transformed into MFI by steaming in the presence of TPA^+. In the technique of Pham *et al.*, a silica support, coated with a layer of 50 nm silica particles, was seeded with b-oriented MFI crystals using the method of rubbing.[5,64] The support was then impregnated with a solution of tetrapropylammonium hydroxide (TPAOH) and tetraethylammonium hydroxide (TEAOH), which can act as structure directing agents for MFI. The SDA-laden support was then sealed in an autoclave and placed in a convection oven at 190 °C. After heating for several hours, the supported membrane was removed, dried, calcined and subjected to permeation testing. As shown in Fig. 3, the silica source for the growth of the zeolite seeds to form a continuous film is provided by the underlying silica nanoparticles. As the authors mention, this method is simple, saves chemicals and most importantly, preserves the orientation and can be scaled up. It is important to note that this method has so far been demonstrated only for silica supports and all-silica zeolite MFI. It should be possible though to extend it to aluminosilicate zeolites, including zeolite A, by use of the appropriate underlayer and support.

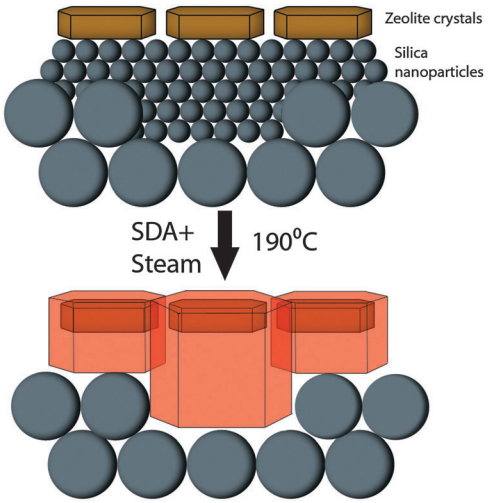

Fig. 3 Schematic of gel-free secondary growth of seeds by consumption of silica nanoparticles to grow zeolite seeds to a continuous membrane. Adapted from ref. 7 with permission from Wiley-VCH.

3.1. Conventional secondary growth and efforts to avoid twinning

Li *et al.* discovered that accurate control of SDA concentration during solution-based secondary growth promotes in-plane growth of MFI crystals and prevents twinning.[65] b-oriented MFI seed layers were first prepared using manual assembly. For secondary growth solutions of composition 1TEOS : *x*TPAOH : $165H_2O$, $0 < x < 0.005$ was found to result in *c*-axis elongated crystals which did not fully intergrow, whereas $x > 0.1$ resulted in a large number of a-oriented twins. At intermediate TPAOH concentration, mostly b-oriented intergrown films of about 400 nm thickness were obtained.

A similar approach to secondary growth was extended to the synthesis of MFI membranes on porous alumina supports.[8] It was proposed that twin crystals could be responsible for membrane defects. Thus the TPA^+/Si ratio was optimized to 0.05 for preventing the formation of twin crystals. This resulted in an EtOH–water selective membrane.

Other developments are the use of microwave heating for aging of growth solution and for secondary growth.[66,67] It is hypothesized that the rapid heating rate by microwave causes a nucleation bottleneck, allowing a compact film to form within 60 minutes without twin formation. For conventional heating, nucleation occurs around 60 minutes, whereas, it requires around 180 minutes or more for the formation of a compact film. This leads to twin formation.

Although numerous reports exist on twin suppression in TPA-based MFI film growth, fundamental understanding is lacking. Also, reproducibility and robustness have not been proven. Secondary growth depends on several factors, including the solution composition, temperature and aging time. Also, the growth procedure has been found to vary based on the type of seed used. For example, the gel-based growth method first reported by Pham *et al.*[5] was used for secondary growth of MFI nanosheet seed layers made by Langmuir trough deposition.[6] However, nanosheets do not grow in the same way as that reported for large bulk MFI crystals. Growth does not uniformly occur with nanosheets, leading to some of the nanosheets growing very fast and others growing very slowly or not at all. This results in a discontinuous film. The same approach when applied to large MFI seeds gives nicely oriented and intergrown films.

The recent work reported by Lupulescu *et al.*[68] indicates that growth of silicalite-1 takes place according to a combination of both classical and non-classical mechanisms. Classical growth mechanisms suggest that growth takes place by the addition of atoms and molecules, as opposed to non-classical mechanisms which hypothesize that growth occurs through attachment of nanoparticles or aggregates.[69] By *in situ* AFM imaging, Lupulescu *et al.* have conclusively shown that initially the increase in height of a silicalite-1 crystal perpendicular to the ⟨010⟩ face happens linearly, in accordance with the addition of molecules. However, after a certain time has elapsed, there is a step-change in the height, which corresponds to nanoparticle attachment. This work may help settle the debate regarding silicalite-1 growth mechanisms and identify conditions for twin-free MFI growth and could be extended towards elucidating the growth mechanisms of other classes of hydrothermally grown zeolites.

3.2. Secondary growth at neutral pH

During membrane synthesis using alumina supports, use of alkaline environment generally causes leaching of Al^{3+} ions and may lead to membrane deactivation. To circumvent this, there have been several reports of using HF to obtain a neutral pH during secondary growth.[36,70] However, the use of HF is undesirable due to the hazards associated with it. Very recently, Peng *et al.* overcame this by using TPABr as SDA and fumed silica as a silica source for secondary growth.[71] The growth is carried out after rubbing MFI seed crystals on glass substrates. The use of glass is crucial because dissolution of Na_2O from glass creates a local mild alkaline environment, allowing growth to proceed. Also, the use of TPABr is beneficial as it is inexpensive compared to the conventionally used TPAOH.

3.3. SDA-free secondary growth

In order to further minimize the use of SDA, several groups have explored the possibility of a seed-assisted synthesis procedure. Some recent reviews summarize the progress towards synthesis of zeolites by such a procedure.[72–75] Here, seeds are first synthesized using SDA and further used for zeolite growth from a sol that is devoid of SDA. There are significant advantages to using an SDA-free synthesis procedure. For large-scale zeolite production, there will be some environmental and economic benefits from eliminating the use of organic SDAs. Most importantly, an SDA-free synthesis approach when applied to membranes will circumvent the final calcination step, which is prone to crack formation due to zeolite shrinkage upon SDA removal. Previously, Xie *et al.* and other research groups have reported the template-free synthesis of beta-zeolite.[76–80] This procedure has been extended to other zeolites, including levyne, EMT and ZSM-5.[81–86]

For membrane applications, this technique has been used to obtain zeolite films on porous supports. Tang *et al.* synthesized MFI membranes on α-alumina supports without using SDA.[87] A H_2/SF_6 separation factor of 1700 and H_2 permeance of 3×10^{-7} mol m^{-2} s^{-1} Pa^{-1} at room temperature was obtained. Wang *et al.* synthesized ~6 μm thick ZSM-5 membranes on porous α-Al_2O_3 supports coated with a YSZ barrier layer (to prevent leaching of aluminum).[88] Zhu *et al.* synthesized template-free ZSM-5 membranes which showed high water perm-selectivity.[89] A H_2O/IPA separation factor of 3100 was obtained during pervaporation of a 10 wt% H_2O–IPA mixture at 70 °C. Recently, this technique was used to obtain supported growth of zeolite beta.[90] Seed-induced hydrothermal synthesis resulted in 3 μm thick *h*0*l* oriented beta membranes on α-Al_2O_3 supports. Pervaporation of a 10 wt% TIPB–ethanol mixture at 30 °C resulted in a total flux of 1.58 kg m^{-2} h^{-1} and an ethanol–TIPB separation factor of 320.

4. Sub-1 μm membrane synthesis

High capital investment and thus long payback times for zeolite membrane separation processes have prevented their large scale implementation. Tsapatsis estimates that one way to reduce the membrane cost to economically viable levels could be by reducing the zeolite membrane thickness to ~50 nm.[12] However, ultrathin membranes, *i.e.*, sub-1 μm thickness of the selective layer, has been an elusive goal for some time in the zeolite community.

As mentioned earlier, Agrawal *et al.* recently obtained 100–200 nm-thick MFI membranes by gel-free secondary growth of 80 nm-thick seed layers consisting of nanosheets (Fig. 4a and b).[11] For 10 membranes made by this method, the permeance for *p*-xylene varied between 1.7–3.6 × 10^{-7} mol m^{-2} s^{-1} Pa^{-1} with a maximum *p*-xylene/*o*-xylene separation factor of 185 at 150 °C. These membranes were also efficient at separating *n*-butane and i-butane, achieving a separation factor of 60 at room temperature with an *n*-butane permeance of 4.3 × 10^{-7} mol m^{-2} s^{-1} Pa^{-1}. At higher temperatures (150 °C), the permeance of *n*-butane went as high as ~13 × 10^{-7} mol m^{-2} s^{-1} Pa^{-1} but the separation factor dropped to 15. The permeances are consistent with the previous report on 200 nm-thick MFI membranes made from nanosheet seeds, but grown using conventional solution-based growth.[10] However, the earlier separation factor of 25–45 for *p*-xylene/*o*-xylene is greatly improved (to >100) by the use of gel-free secondary growth. Other efforts for ultrathin MFI membranes are discussed below.

Recent developments by Sjöberg *et al.* have led to the synthesis of sub-micron MFI zeolite membranes. A 0.7 μm think MFI membrane was used to separate CO_2 from the synthesis gas (or syngas) derived from black liquor, a byproduct of the paper processing industry.[91] Typically, syngas from black liquor has high CO_2 and H_2S and must be ''sweetened'' by removal of these gases. The authors synthesized MFI membranes by first masking the α-Al_2O_3 flat supports. The masking process results in impregnation of the support with wax and prevents invasion of the synthesis solution into the support pores and subsequent leaching.[92] The masked supports were seeded and intergrown to form a 0.7 μm MFI film. The use of such thin films results in a very high CO_2 permeance of 11.0 × 10^{-7} mol m^{-2} s^{-1} Pa^{-1} at 2.25 MPa feed pressure and 0.3 MPa permeate pressure at room temperature. However, the CO_2 permeance reduces to almost half this value after 10 hours of testing, due to competitive adsorption of H_2S. This also causes the CO_2/H_2 separation factor to decrease from 10.4 to 5.0. Thus these membranes are only suitable for feed with small quantities of H_2S.

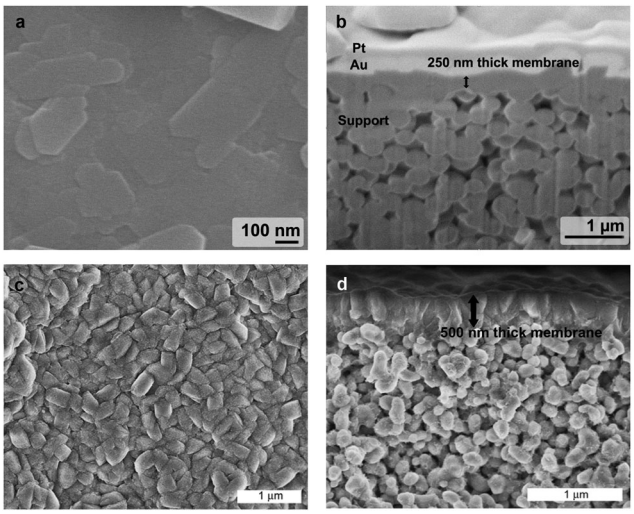

Fig. 4 (a): Top view SEM image of 250 nm MFI membrane made by gel-less secondary growth, (b): cross-sectional SEM image of membrane shown in (a). (c): Top view SEM image of 0.5 μm MFI membrane made by the masking method followed by secondary growth, (d): cross-sectional SEM image of membrane shown in (c). (a), (b) reprinted from ref. 11 with permission from Wiley-VCH. (c), (d) reprinted from Danil Korelskiy, Tiina Leppäjärvi, Han Zhou, Mattias Grahn, Juha Tanskanen, Jonas Hedlund *J. Membr. Sci.*, 2013, **427**, 381–389 (ref. 9). Copyright 2013, with permission from Elsevier.

In another recent work,[9] a similar method to the one described above was used for the synthesis of 0.5 μm thick MFI membranes for the separation of alcohol and water by pervaporation (Fig. 4c and d). The fluxes obtained for the separation of 3 wt% *n*-butanol–water and 10 wt% ethanol–water mixtures were the highest reported in the literature. However, the alcohol/water separation factors were low (4–5) at 30 °C. This was attributed to the support favoring the transport of water due to Knudsen diffusion. The separation factor for the membrane alone was calculated to be almost 50% higher. The authors conclude that to improve both flux and selectivity, the support resistance needs to be reduced – a general challenge for achieving high flux membranes from thin zeolite films.

The same group also investigated the separation of *n*-butanol and water in the vapor phase by using a hydrophobic MFI membrane.[93] The supports were first seeded (without masking) and intergrown using a synthesis solution containing TPAOH and HF. The final membrane thickness was found to be 0.5 μm. Permporometry experiments using *n*-hexane indicated that the defects in this membrane were almost half that of the

membrane synthesized using conventional synthesis sol. For the separation of 50/50 mol% *n*-butanol/water, the hydrophobic MFI membrane had an *n*-butanol permeance of 7×10^{-7} mol m^{-2} s^{-1} Pa^{-1}, which was half that of the conventional MFI membrane at 160 °C. However, the separation factor (8.3) of the former was twice that of the latter. The lower permeance and higher separation factor of these membranes were attributed to higher hydrophobicity and lower defect density.

The use of hydrophobic MFI membranes was further extended to CO_2/H_2 and CO_2/CO separations.[36] In this case as well, a 0.5 μm membrane was obtained which was confirmed to be b-oriented by X-ray diffraction. The orientation as well as the use of HF for synthesis served to reduce defects even further to 0.13% of membrane area. A CO_2/H_2 separation factor of 100 was obtained at −35 °C and it decreased with increasing temperature. The CO_2/CO separation factor was 20 at −15 °C. The CO_2 permeances remained very high, in the range of $50–60 \times 10^{-7}$ mol m^{-2} s^{-1} Pa^{-1}.

As selective zeolite films become very thin, a number of challenges emerge. Transport may be dominated by pore entry resistance rather than intracrystalline transport and this may alter the transport behavior compared to that of thicker membranes. Also, the development of supports that offer low resistance to permeation is required.

5. Spatially resolved permeance characterization of membranes

An important recent advancement in the study of defects is the use of a mass spectrometer probe to spatially resolve gas permeances through tubular membranes.[94] These studies build on earlier reports on membrane characterization by measurement of the local He permeance.[95,96] SAPO-34 membranes were synthesized on the inner surface of alumina tubes by a seeded hydrothermal synthesis. Either CO_2 or CH_4 was fed on the outer surface of the membrane and a silica capillary connected to a mass spectrometer was used for collecting the permeate at the inner surface of the membrane, as seen in Fig. 5. This method allowed determination of permeances with good angular and lateral resolution. The authors determined that the permeance of CO_2 and CH_4 is not uniform. The presence of defects was measured by using i-butane, which has a kinetic diameter of 0.5 nm and is too large to fit in the 0.38 nm SAPO-34 pores. Any area with high i-butane flow could be assumed to have a defect larger than 0.5 nm. The defects did not contribute to a change in CO_2 permeance in those regions because of the high permeance of CO_2 at low pressures. However, at high pressures the influence of defects could become important.

Spatially resolved permeance characterization also enabled the improvement of the synthesis of SAPO-34 membranes. Impermeable regions, in which the synthesis gel remained after the synthesis, could be detected.[97] By increasing the membrane rinsing time, spatially uniform membranes with high permeance could be obtained. The synthesis was subsequently improved by eliminating almost all defects larger than 0.47 nm.[98] Seeds were deposited on the inner surface of tubular alumina supports by manual rubbing. The gel composition used for growth was $0.85Al_2O3 : 1.0P_2O_5 : 0.3SiO_2 : 2TEAOH : 155H_2O$, with $Al(OH)_3$ as an alumina source. Membranes prepared by this method achieved a CO_2/i-butane selectivity of 15 000 to 20 000 and a CO_2/CF_4 selectivity of 12 000 to 20 000 at pressures up to 0.5 MPa. These are the highest reported selectivities for zeolite membranes. High CO_2 permeance (on the order of 10^{-6} mol m^{-2} s^{-1} Pa^{-1}) and CO_2/CH_4 selectivity on the order of 100 at room temperature and low feed pressure were also obtained.

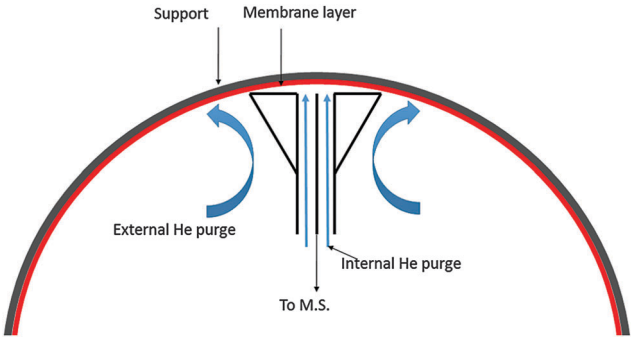

Fig. 5 Schematic of mass spectrometer probe for permeance characterization. Reprinted from H. H. Funke, B. Tokay, R. Zhou, E. W. Ping, Y. Zhang, J. L. Falconer and R. D. Noble, *J. Membr. Sci.*, 2012, **409–410**, 212–221 (ref. 94). Copyright 2012, with permission from Elsevier.

6. Polymer supported membranes

Since the overall cost of membranes is determined in large part by the support cost, it is desirable to develop inexpensive polymeric supports. This would overcome the current limitations of ceramic membranes, including their high failure rate and cost of manufacture. In addition to being less expensive per unit area, membranes supported on polymeric hollow fibers would also be able to pack better, giving higher membrane area per unit volume.[99]

Mixed matrix membranes combining polymers with zeolites have long been studied extensively aiming at low-cost, high-performance membranes.[100–108] (see also Section 13). However, the inherent incompatibility between zeolites and polymers still remains a limitation, while performance of these membranes has remained low to modest at best.

MOFs, generally, appear to have better compatibility with polymers in mixed matrix membranes compared to zeolites.[109–111] However, performance gains have been similarly modest. Even if compatibility is resolved there are other issues like the flux matching requirement which allow only a small fraction of the zeolite/MOF selectivity to be harvested in a mixed matrix setting.[112] For this reason, deposition of a continuous zeolite deposit on or in a porous support is more desirable.

Following this approach, Wang, Yan and co-workers have fabricated high-flux composite hollow fibers (CHF) consisting of zeolite NaA and polyethersulfone (PES).[113] Two different

sizes (4.0 μm and 1.5 μm) of zeolite particles were combined with the polymer solution in different concentrations and extruded through a spinneret. Zeolite membranes were prepared on the external support of the CHFs by a hydrothermal process. It was found that increasing the loading of zeolite in CHF led to more void spaces and agglomeration of crystals, thus increasing the CHF porosity. The larger zeolite particles led to CHFs with lower porosity. At 85 wt% zeolite loading the difference between the two particle sizes becomes small and dense zeolite coverage is obtained. At this loading, 4–5 hours of growth time give a high flux membrane for water–ethanol separation. For pervaporation of 90 wt% EtOH–H_2O feed at 70 °C, a flux of >10 kg m^{-2} h^{-1} is obtained with a H_2O/EtOH separation factor of $>10\,000$.

These types of membranes were further improved by having the membrane on the inner surface of zeolite/PES-PI hollow fibers.[114] The addition of PI (polyamide) gives added temperature resistance and mechanical strength. Membranes on the inner surface help to prevent damage to the selective zeolite layer. Similar EtOH–H_2O pervaporation performance was obtained as in the previous report. However, the fibers with higher mechanical and bending strength and with membranes on the inner surface are significant improvements, which could enable commercialization of this technology in the future.

Synthesis of zeolite membranes on flat polymeric supports was also reported recently.[115] Faujasite membranes were synthesized on PES supports supported on a polyester backing. A continuous FAU membrane with a thickness of 500–700 nm was fabricated using just 1 hour of hydrothermal growth on seeded PES supports. The synthesis was further improved so that a 300 nm thick FAU membrane could be obtained on flat PES supports.[116] After elimination of intercrystalline defects by using a PDMS coating (see Section 7), CO_2/N_2 selectivities of $\sim$72 could be obtained.

As it will be described in more detail in Section 11 of this review, polymer supports and MOFs match very well since usually for MOF activation only the remaining solvent molecules have to be removed at temperatures <100 °C. That is to say, in the case of MOF activation, no structure directing agent/template molecules have to be removed by burning in air at 450–500 °C. Anyway, because of the organic linkers, no MOF would survive this harsh treatment. There are some recent promising reports of MOFs on polymer supports. Brown *et al.* synthesized a ZIF-8 layer in a series of poly(amide–imide) (Torlon) hollow fibers by interfacial microfluidic processing.[117] The interfacial synthesis method was also used by Li *et al.* to prepare a ZIF-8 membrane layer on a porous polyethersulfone as a support[118] and by Campbell *et al.* who produced a thin HKUST-1 layer on porous polyimide ultrafiltration supports. Cacho-Bailo *et al.* synthesized ZIF-7 and ZIF-8 membranes on the inner surface of a polysulfone hollow fiber using microfluidics.[119]

7. Post-synthesis modification

There are several reports on post-synthesis techniques for improving membrane performance. It has been shown early on that post-synthetic coking of MFI membranes by impregnating and then pyrolyzing TIPB can be used to plug macro voids and defects between zeolite crystals.[120] This causes a remarkable increase in the *n*-butane/i-butane selectivity but causes reduction in permeance. In some cases, membranes have been subjected to a UV or thermal treatment, to either cause cross-linking of the polymer matrix in composite membranes or to seal defects in the zeolite layer.[121,122] In other cases, membranes have been post-synthetically treated with chemicals such as oxalic acid, which causes the membrane selectivity to increase.[123]

CVD modification is another widely used post-modification technique. Nomura *et al.* applied the counter diffusion CVD technique in which TEOS and ozone cause amorphous silica to deposit on the membrane.[124,125] This plugs the intercrystalline defects without completely plugging the zeolite pores as TEOS is too large to enter them. A similar TEOS–O_3 system was used recently for plugging of defects in porous silica membranes of pore size $\sim$1 nm.[126]

Lin and co-workers have used the CVD technique for post-synthesis modification of MFI and DDR-type membranes.[88,127–129] For small non-adsorbing molecules like H_2 and CO_2, the transport is governed by Knudsen diffusion. Thus, plugging of large intercrystalline defects by CVD using a molecule like methyldiethoxysilane (MDES) or TEOS increases the H_2/CO_2 separation factor. However, this is true only for membranes with good initial quality, *i.e.* those lacking large intercrystalline voids.

Apart from CVD, catalytic cracking deposition (CCD) of MDES was also used in order to reduce the pore size of MFI and effect better separation of H_2 and CO_2.[88] CCD causes deposition in the pores of zeolite and thus reduces H_2 permeance of a ZSM-5 membrane by an order of magnitude (from 2.2×10^{-7} to 0.6×10^{-7} mol m^{-2} s^{-1} Pa^{-1} at 450 °C). However, the H_2/CO_2 separation factor increases from about 5 to 19.1. Tang *et al.* improved on this work by obtaining a H_2/CO_2 separation factor larger than 100 at 450 °C and 1.5 bar feed pressure.[130] CCD of MDES only causes a slight decrease in the H_2 permeance (from 3.75×10^{-7} to 2.2×10^{-7} mol m^{-2} s^{-1} Pa^{-1}).

However, the limitations of CVD and CCD post-treatment are the expensive equipment and difficulty in scaling up. Moreover, amorphous silica deposits are known to undergo densification upon prolonged heating, especially in the presence of water vapor.[131] Therefore, the long term stability of these membranes is uncertain.

An alternative approach is the use of a permeable polymer like polydimethyl siloxane (PDMS) to seal membrane defects.[132] CO_2/N_2 separation factors of >1000 at 130 °C are reported after application of a 150 nm PDMS top layer to silica and zeolite Y membranes. The only limitation of using PDMS is that the temperature has to be limited to 250 °C. Fluoropolymers or other temperature resistant polymers may be able to overcome this limitation, provided that they can be made sufficiently permeable.

A post-synthesis modification that improves the hydrophobic properties of the membranes is using silylation. It is known that treatment of zeolites or silica surfaces with triethoxyfluorosilane

(TEFS) converts surface silanol groups to Si–F groups, thus increasing the hydrophobicity.[133,134] Use of TEFS is advantageous over carbon-based silanes due to decomposition of the latter leading to re-formation of silanol groups upon calcination.[135] Recently, Kosinov *et al.* showed that the treatment of high silica MFI and MEL membranes (Si/Al ~ 100) improves the ethanol/water separation performance.[136] The best performing membrane had an EtOH/water separation factor of 34 and a flux of 1 kg m^{-2} h^{-1} after treatment with TEFS twice. There is only a marginal reduction of flux (1.5 kg m^{-2} h^{-1} initially) indicating that TEFS mainly modifies the membrane surface and retains the porosity.

The organic nature of MOFs allows a wealth of post-synthesis modifications. Here, we only refer to a recent review by Qiu *et al.* on the synthesis and application of MOF membranes including their post-synthesis modification.[137]

8. Modeling permeation through zeolite membranes

The Maxwell–Stefan approach provides a fundamental description of multi-component diffusion. Krishna and co-workers have extended this approach to formulate the generalized Maxwell–Stefan model for surface diffusion of adsorbed species in a zeolite membrane.[138–143] Permeation through a zeolite membrane is a combined effect of adsorption and diffusion characteristics. The influence of adsorption is taken into account through the fractional loading at the surface and the thermodynamic factors while the mobility is determined by the two kinds of diffusion coefficients – the corrected diffusivity which is also known as Maxwell–Stefan diffusivity and the exchange coefficients. One of the advantages of using these equations is that the mixture adsorption and diffusion parameters, for most of the cases, can be obtained using only pure component data.[141]

8.1. Adsorption

The pure component adsorption isotherm is most commonly modeled using the dual site Langmuir model.[144,145] Other forms of the isotherm *e.g.* Toth, Langmuir–Sip, Langmuir–Freundlich have also been used.[146–148] The mixture isotherm can be predicted, from the pure component isotherm, by implementing appropriate mixture rules.[149] However, the use of mixture rules is only moderately successful and a thermodynamically consistent model, known as Ideal Adsorption Solution (IAS) theory,[150] is widely used for predicting mixture isotherms from pure component data. Fig. 6a shows that the prediction of IAS theory for a mixture of alkanes is in excellent agreement with simulation results.[151] One of the drawbacks of IAS theory is the assumption that the system behaves like an ideal solution and therefore, it is inadequate to describe multicomponent adsorption for non-ideal mixtures. The existence of non-idealities in the mixture is either due to energetic or surface heterogeneity or due to a non-ideal mixture itself. Energetic heterogeneity arises due to varying heat of adsorption for different sites while surface heterogeneity is caused due to different surface area (sites) available for adsorption of different species. Various extensions of IAS theory have been described to account for these non-idealities. Heterogeneous IAS theory has been used to account for energetic heterogeneity[152] and surface area corrected IAS (SAC-IAS) theory has been used to account for surface heterogeneity.[153]

The presence of non-idealities in the mixture can also lead to failure of IAS theory as shown in Fig. 6b for water–ethanol mixture in MFI zeolite.[154] Non-ideal behavior arises due to hydrogen bonding between molecules. Such deviations from ideality are captured by using a more general theory than IAS, known as real adsorption solution (RAS) theory.[150] The RAS theory makes use of the activity coefficients to account for these deviations; these coefficients are, in general, functions of temperature, composition and spreading pressure but the dependence on spreading pressure is often neglected due to complexities. Thus the activity coefficient models such as UNIQUAC, NRTL and Wilson, which are used to describe vapor–liquid equilibrium, are often applied with good accuracy to the mixture adsorption as well.[155–159] The parameters are obtained by fitting the experimental or simulation data.

8.2. Diffusion

The corrected diffusion coefficient accounts for sorbate–sorbent interactions and exhibits loading dependency. Various models

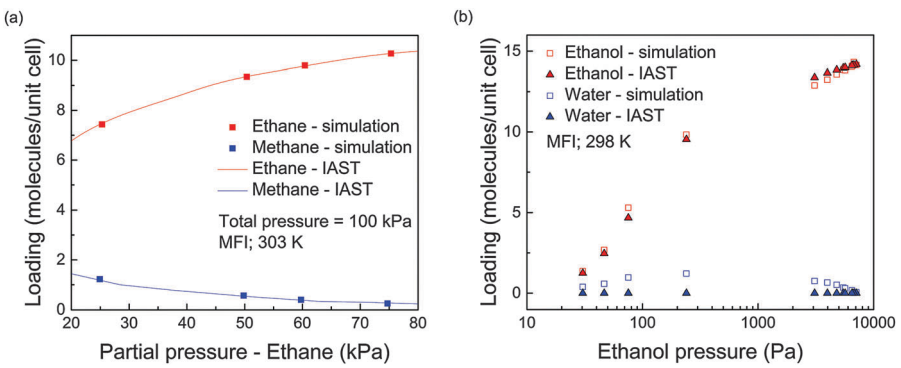

Fig. 6 Molecular simulation results and IAST prediction for multicomponent adsorption on MFI crystals: (a) success of IAST for methane–ethane mixtures (adapted from R. Krishna and D. Paschek, *Sep. Purif. Technol.*, 2000, **21**, 111–136 (ref. 151). Copyright 2000, with permission from Elsevier. (b) failure of IAST for water–ethanol mixture. Adapted from P. Bai, M. Tsapatsis and J. I. Siepmann, *Langmuir*, 2012, **28**, 15566–15576 (ref. 154). Copyright 2012, with permission from the American Chemical Society.)

have been used to predict this loading dependency. The most commonly used are the weak confinement scenario and the strong confinement scenario, which are based upon the vacancy factor and the repulsion factor.[160] The vacancy factor accounts for the probability of the adjacent adsorbing site being vacant and decreases with loading while the repulsion factor accounts for inter-molecular repulsion and increases with loading. However, these are the ideal scenarios and the actual dependency varies between the two scenarios (see Fig. 4 in ref. 160). Another model, based upon the quasi-chemical approach of Reed and Ehrlich, also accounts for the reduction of the energy barrier for diffusion with increased loading and is also widely used.[161,162] Since the corrected diffusivity is interpreted in terms of hopping from one adsorbed site to another, the loading dependence is strongly influenced by adsorption thermodynamics. It has been shown that the corrected diffusivity is inversely proportional to the thermodynamic factor which signifies the change in fractional loading with respect to a change in fugacity and can be calculated from the adsorption isotherm.[163–165] The corrected diffusion coefficient of a species in a mixture is usually taken equal to that of the pure component at the same total loading.

The exchange coefficients account for sorbate–sorbate interactions and capture the effect that a faster moving molecule is slowed down in the presence of slower moving species and *vice versa*.[166] The incorporation of the exchange coefficients into the Maxwell–Stefan equations leads to computational difficulties and thus are often neglected; this scenario is known as the facile exchange.[140,160] However, these effects have been shown to be significant and various models have been proposed for their incorporation.[167,168] Vignes correlation for species with similar loading and the Sholl correlation for species with variable loading are the two most commonly used models.[160] Since the exchange coefficients capture the sorbate–sorbate interactions, it has also been found that there is a dependence of the exchange coefficients on the corresponding fluid phase diffusivity; the proportionality factor depends upon the degree of confinement and the correlation effect increases with the degree of confinement.[169] The factor is often linearly dependent upon the degree of confinement, however, other expressions such as Darken-type interpolation and Vignes-type interpolation have also been proposed.[169]

8.3. Predictions

The Maxwell–Stefan approach using the above discussed models for adsorption and diffusion have been proven to be very useful in predicting the separation performance of zeolite membranes and also verified against experimental and molecular simulation results.[170–172] The key to success for the Maxwell–Stefan model is the accurate determination of multi-component adsorption and diffusion characteristics of the permeating species. Though these equations have provided a deep insight into the permeation through zeolite membranes, there are cases for which the Maxwell–Stefan model fails to interpret the experimental results. This is either due to the fact that the assumptions used for predicting multi-component adsorption and diffusion characteristics are not adequate or due to some other factors which are discussed next.

One of the examples where the Maxwell–Stefan model fails to provide quantitative agreement with the experimental results is the xylene isomer separation using MFI zeolite membranes. The adsorption and diffusion characteristics of *p*-xylene and *o*-xylene in MFI crystals have been extensively studied and the adsorption parameters and the diffusion coefficients have been extracted from the experimental results.[173–176] The permeation of xylene isomers was also studied using Maxwell–Stefan equations. Though the permeance of *p*-xylene has been observed to be of the same magnitude, the Maxwell–Stefan model predicts much higher *o*-xylene permeance as compared to the experiments (see Fig. 5 in ref. 175). This discrepancy may be attributed to surface resistances in zeolite crystals or to the changes in crystal structure on adsorption of *p*-xylene.[175,177] It can also be due to the fact that the diffusion coefficient used in the Maxwell–Stefan equations was measured for a flexible zeolite crystal while an intergrown supported membrane is constrained by a support and does not permit flexibility, as in the case of a free crystal. Another phenomenon where the Maxwell–Stefan approach fails is the intersection blocking.[178] It is usually observed when branched or cyclic hydrocarbons are present in the mixture along with linear hydrocarbons in MFI. The branched hydrocarbon preferentially adsorbs at the intersection of MFI membranes which causes blocking of the pore and severely reduces the diffusivity of the normal alkane.[145] In general, the tardy species slows down the fast moving species and the effects are captured by the exchange coefficients but this effect is more severe and can cause the diffusivity of *n*-alkane to reduce nearly to zero. The effect of intersection blocking for methane in the presence of i-butane is shown in Fig. 7a. The reduction in diffusivity is more severe as compared to the methane–*n*-butane mixture, which does not have intersection blocking.[178] Similarly, the Maxwell–Stefan equations fail to interpret the experimental results for permeation of *n*-hexane–3-methylpentane across a MFI membrane.[179]

In mixtures governed by hydrogen bonding or molecular clustering effects, the adsorption and diffusion coefficients cannot be obtained by using only the pure component data.[180] As already discussed, IAS theory leads to a higher separation factor for water–alcohol separation as the adsorbed alcohol molecules also bring the water molecules into the zeolite due to hydrogen bonding.[154] The corrected diffusion coefficient for such systems also depend upon the mixture composition along with the total loading as shown in Fig. 7b.[148,181] The correlation effects are also stronger than Vignes interpolation. One peculiar characteristic of such mixtures is the mutual slowing down of both permeating species.[182,183] Thus, using the pure component data to predict the separation performance will lead to higher predicted flux and higher separation factors than experimentally feasible.[184–186]

8.4. Effect of impurities

Another concern for industrial application of zeolite membranes is the presence of impurities. It has been shown that a strongly adsorbed component, even present in small quantity, can suppress the flux of other components and affect the

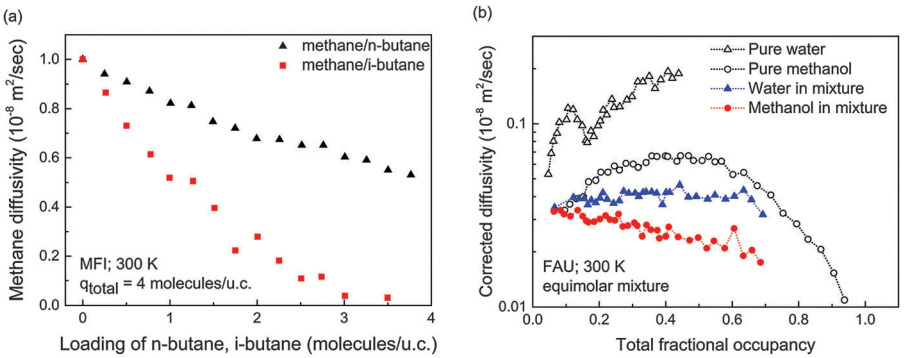

Fig. 7 (a) Effect of intersection blocking: diffusivity of methane (linear alkane) decreases more steeply in the presence of i-butane (branched alkane) as compared to *n*-butane (linear alkane) in MFI (Adapted from R. Krishna and J. Baten, *J. Eng. Chem.*, 2008, **140**, 614–620 (ref. 178). Copyright 2008, with permission from Elsevier), (b) corrected diffusivity of water–methanol mixtures in FAU at 300 K obtained through MD simulations. (Reprinted with permission from adapted from R. Krishna and J. M. van Baten, *Langmuir*, 2010, **26**, 10854–10867 (ref. 148). Copyright 2010, with permission from the American Chemical Society.)

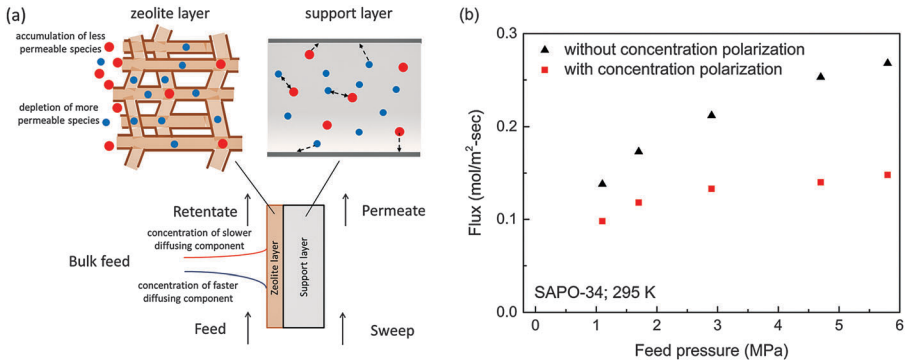

Fig. 8 (a) Schematic of concentration polarization for permeation through a zeolite membrane, (b) effect of concentration polarization: CO_2 flux through a SAPO-34 membrane for an equimolar mixture of CO_2/CH_4 at 295 K. Reprinted from A. M. Avila, H. H. Funke, Y. Zhang, J. L. Falconer and R. D. Noble, *J. Membr. Sci.*, 2009, **335**, 32–36 (ref. 200). Copyright 2009, with permission from Elsevier.

separation performance.[187] Similar degradation in the separation performance of CHA zeolite membranes has been observed when propane is introduced in the separation of CO_2/CH_4 and N_2/CH_4 mixtures.[188]

8.5. Other factors

Apart from these challenges, some other factors can significantly affect the separation performance of the membranes. These include the effect of the porous support, sweep gas and concentration polarization.

The zeolite membranes are usually supported on a porous support. The support layer is usually neglected in most of the modeling studies. However, it has been shown that the support can play a significant role especially in thin or high-flux membranes.[189,190] The significant mass transfer resistance in the support adversely affects the separation performance of MFI and FAU membranes for ethanol/water separation.[9,191] The effect is more prominent for strongly adsorbing species as shown for H_2/CO_2 separation where the pressure drop for CO_2 over the support was quite large and influenced the separation performance.[192] Thus, flux and selectivity for high flux membranes can be increased by preparing less resistive supports. It is essential to incorporate transport resistance effects due to the support layer in permeation models. The models proposed in the literature are well established and incorporate flux through the Knudsen and bulk diffusion and viscous flow.[144,193,194]

The sweep gas is introduced to carry away the species on the permeate side and thus increase the driving force for permeation. In most of the modeling studies, the effect of sweep gas is incorporated by assuming zero partial pressure of the species on the permeate side. However, it has been shown that the rate of flow of sweep gas can play a significant role.[195] The sweep gas increases the driving force for the permeating species and enhances the separation performance. This effect has been shown for methane/ethane separation.[196] A negative effect on the permeation can occur due to the counter flux of the sweep gas. A higher pressure of helium on the permeate side increases its counter flux and thus decreases the permeance of ethane.[197]

Selective permeation usually shifts the adsorption equilibrium at the membrane surface and thus reduces the separation factor.[198] This effect is known as concentration polarization and is depicted through a schematic in Fig. 8a. Though not many modeling studies of zeolite membranes consider the concentration polarization effect, it can play a significant role.[199,200]

It has been shown that the CO_2/CH_4 selectivity increased by 180% and CO_2 flux by 80% when measures were taken to reduce the external boundary layer resistance for a SAPO-34 membrane, as shown in Fig. 8b.[200] The effects of concentration polarization are more prominent for pervaporation as compared to gas permeation since the diffusion coefficient is higher for gases. Various models have been proposed in the literature to include its effect by introducing a mass transfer coefficient,[192,201,202] or solving the full concentration profile in the boundary layer.[203,204] The effects can be suppressed by introduction of sweep gas, mixing and making flow turbulent.

Another common assumption in modeling zeolite membranes is that they are defect free. However, it has been illustrated that the defects can significantly affect the separation performance in H_2/CO_2 separation,[192] xylene and butane isomer separation.[205] It has also been shown that defects can be induced and shrunk or expanded during adsorption and affect the permeation.[177] Permporometry, flux of molecules larger than zeolite pores and the ratio of single gas permeance, and other methods have been used to characterize defects.[206–209] These effects have been incorporated in some of the modeling studies by determining the permeation through the defects as a combination of Knudsen diffusion and Poiseuille flow.[210,211] A general pore network model has also been developed to account for the flux through intercrystalline pores.[212]

8.6. High throughput computational screening of zeolite structures

By using this technique, a library of structures consisting of several thousands of structures can be rapidly screened based on desirable attributes. These could include pore size, adsorption properties and gas separation performance. A recent review summarizes the work that has been done so far on high throughput screening of MOF structures.[213]

Two important factors for the characterization of porous networks are the largest cavity diameter (LCD) and the pore limiting diameter (PLD). The LCD gives an estimate of whether two molecules of different species can pass each other within the structure. This is useful for separations. If a molecule's size is smaller than the PLD, it can diffuse freely through the network. If not, there is a significant energy energy barrier towards diffusion. Haldoupis *et al.* characterized $>250\,000$ hypothetical zeolite frameworks based on their PLD and LCD.[214] First *et al.* characterized the existing zeolite frameworks with respect to the accessible pore volumes, surface areas, PLDs and LCD.[215]

First *et al.* also screened 196 zeolite frameworks and 1690 MOF frameworks to find candidate structures for gas separations such as CO_2/N_2, CO_2/CH_4, CO_2/H_2 and hydrocarbons such as propane/propylene and ethane/ethylene.[216,217] The screening was based on the calculation of the shape selectivity of the framework for the gases of interest using a minimum-energy pathway approach.

Martin *et al.* developed a method for computational screening of zeolite structures for adsorption-based separations such as CO_2/N_2.[218] The Henry coefficient (K_H) and heat of adsorption (H_A) were computed through Monte Carlo simulations for about 140 000 structures. Those with the highest K_H and H_A for CO_2 were screened as possible candidates for CO_2/N_2 separation. This technique of selection was a large improvement (60–70 fold enrichment of possible structures) over the previous random selection or brute-force approaches.

Kim *et al.* screened the experimentally verified IZA structures and 30 000 hypothetical structures for ethane/ethene separation.[219] They found about 30 potentially high-performing structures for this separation. Other studies have used computational screening to identify possible candidates for CO_2/CH_4, CO_2/N_2 separation,[220] natural gas purification,[221] ethanol purification from fermentation broths and hydroisomerization of alkanes.[222]

9. Progress in industrial application of zeolite membranes

The review by Gascon *et al.* highlights the progress made on synthesis and application of zeolitic membranes and coatings during the last few years.[1] However, so far only one type of zeolite membrane has been commercialized. LTA membranes are used in the dehydration of different solvents because of their strong hydrophilicity and suitable pore size. There is still no gas separation process worldwide in operation using zeolite membranes. Ambitious aims for the development of an industrial process for xylene isomer[92] and butene isomer[223] separation using MFI membranes could not be realized yet. Despite excellent lab test results and successful scale-up work, the industrial installation of SAPO-34 and DD3R membranes in the CO_2/CH_4 separation could not be realized either.[224–226]

The established technology for the production of dry (bio) ethanol is the pressure swing adsorption (PSA) using 3 A zeolite (K^+ exchanged LTA).[227,228] Polymers are of interest for replacing PSA by a membrane technology, since they have advantages over inorganic membranes such as lower production costs, easy manufacture and scale up.[229] Especially polyimides and polyamide-imides turned out to be promising pervaporation membrane materials because of high separation performance, low swelling and excellent thermal, chemical and mechanical stability.[230–232]

A pioneering role in the development of zeolite Na-LTA zeolite membranes for the dehydration of bio-ethanol was played by Bussan Nanotech Research Institute Inc. (BNRI), Japan, a Member of the Mitsui Holding, which developed a process for the production of fuel-grade ethanol by a hybrid distillation/vapor permeation process.[233,234] Further milestones in the development of commercial LTA membranes for de-watering of different liquids by pervaporation are the advancements of BNRI,[235] Inocermic GmbH, Germany (ethanol[236]), Smart Chemical Company (*t*-butanol[237] and tetrahydrofuran[238]), Nanjing Jiusi Hi.Tech Co. (different solvents), and a 100% daughter of Dalian Institute of Chemical Physics working for Jiangsu Xinhua Chemical Co. Ltd (mainly i-propanol, but also other solvents).[239]

In this review, the Chinese activities will be highlighted since the Nanjing and Dalian teams have so far established

Fig. 9 Apparatus for dehydration of ethanol (1500 tons per year), left, apparatus for dehydration of acetonitrile (15 000 tons per year), right above, and membrane modules for dehydration, right below, at Jiangsu Nine Heaven High-Tech Co. Ltd (from ref. 243).

over 50 plants for dehydration of industrial solvents from the chemical and pharmaceutical industry in China. The separation systems concern methanol, ethanol, isopropanol, acetonitrile, tetrahydrofuran, MTBE, ethylene glycol *etc.* Recently, the more stable zeolite T (erionite–offretite) membranes[240,241] came into the focus.

A combined seeding method by using ball-milled seeds was developed at Nanjing University of Technology for the synthesis of LTA zeolite membranes, which could improve reproducibility and reduce synthesis time significantly.[242] In 2011, the Jiangsu Nine Heaven High-Tech Co. Ltd was founded as a spin-off, to promote the commercial application of the LTA membrane dehydration technique. A production line of LTA zeolite membranes with the productivity of 10 000 m^2 per year has also been established. The NaA zeolite membranes are prepared on the outer surfaces of home-made 80 cm long mullite supports.

Fig. 9 shows an industrial apparatus for the dehydration of ethanol (1500 tons per year) from 93 wt% to 99.5 wt%.[243] It has 7 membrane modules connected in series with each module having a membrane area of 3 m^2. The apparatus is operated under the vapor permeation mode. A significant reduction (over 50%) in the separation cost was achieved for the membrane technique instead of extractive distillation with salt. The lifetime for the membranes used in the system is more than two years. Fig. 9 also shows an apparatus for dehydration of acetonitrile (15 000 tons per year) from 80 wt% to 99 wt%. The apparatus has 20 membrane modules (10 m^2 per each) with a total membrane area of 200 m^2. The membrane dehydration technique can save more than 50% steam consumption for the production of acetonitrile compared with rectification under vacuum.

In 2012, Dalian Institute of Chemical Physics (DICP) installed at Jiangsu Xinhua Chemical Co. Ltd an LTA zeolite membrane unit for i-propanol dewatering with a capacity of 50 000 tons per year. The separation unit consists of 35 modules with a total permeation area of about 350 m^2 (Fig. 10) which is the largest zeolite membrane facility in the world.[244] This progress of the researchers at DICP is mainly due to the

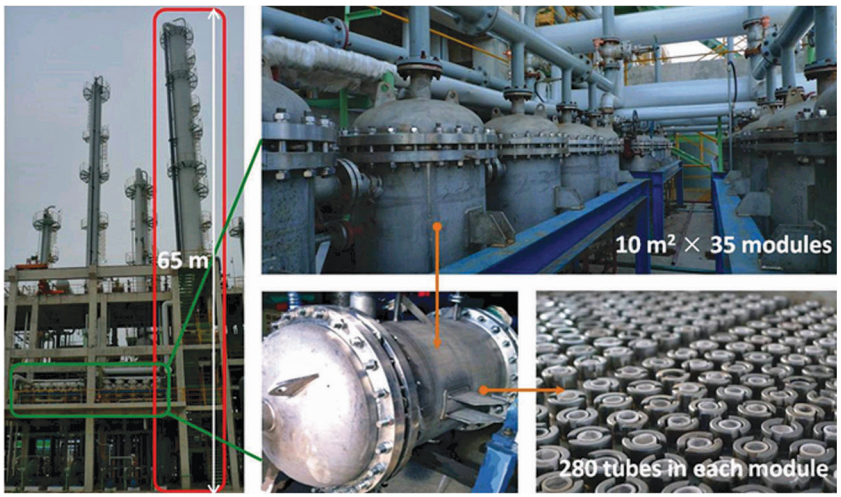

Fig. 10 DICP plant with LTA zeolite membrane units for a capacity of 50 000 tons per year for i-propanol dewatering for Jiangsu Xinhua Chemicals Co. Ltd. The membrane unit (in the green frame) replaces the distillation column (in red frame) achieving reduction in energy consumption. Reprinted from Y. S. Li and W. S. Yang, *Chinese J. Catal.*, 2015, **36**, 692–697 (ref. 239). Copyright 2015, with permission from Elsevier.

use of microwave heating.[245–249] Microwave heating does not only reduce synthesis time, but it also appears to reduce the formation of non-zeolitic defect pores in comparison with conventional heating.[250]

10. Zeolite membrane reactors for the intensification of chemical processes

During the last 5 years, a few comprehensive reviews on zeolite membrane reactors appeared.[251,252] Membrane reactors are one of the concepts for intensified chemical processes.[253] A (catalytic) membrane reactor combines a chemical reaction with an *in situ* separation in one unit.[254–256] Catalytic membrane reactors can be classified according to their function into (i) extractor-, (ii) distributor-, and (iii) contactor-type reactors. The extractor mode especially requires a high separation selectivity, which can be provided by zeolitic molecular sieve membranes. In addition to their molecular sieving function, zeolite membranes are relatively stable at the temperatures of most chemical reactions and they are stable against solvents in comparison with organic polymer membranes. In the past, there were numerous examples of increase in yield of a dehydrogenation or esterification reaction if the product molecules, hydrogen or water, respectively, could be removed selectively under equilibrium-controlled reaction conditions from the product mixture.[257]

Here, the progress after 2010 is reviewed. There are increasing activities to develop hydrophilic water-selective membranes which are more stable than LTA. Zeolite SOD is hydrophilic like LTA, but with a higher framework density of 17.2 T/1000 Å^3, it shows a higher chemical and thermal stability compared with zeolite LTA (12.9 T/1000 Å^3).[258] The small pore size of the 6-ring of H-SOD (2.65 Å) allows molecular sieving, *i.e.* the selective permeation of small molecules like H_2O with kinetic diameters of 2.6 Å. Therefore, due to their hydrophilicity and molecular sieving properties, SOD membranes can accomplish the removal of steam under harsh reaction conditions[259–261] and could be used in the synthesis of methanol (MeOH, eqn (1)), dimethylether (DME, eqn (2)) and dimethylcarbonate (DMC, eqn (3)) in catalytic membrane reactors with carbon dioxide, hydrogen or methanol as reagents:[262]

$$CO_2 + 3H_2 \leftrightarrows CH_3OH + H_2O \quad (1)$$

$$2CO_2 + 6H_2 \leftrightarrows CH_3OCH_3 + 3H_2O \quad (2)$$

$$CO_2 + 2MeOH \leftrightarrows CH_3OCOOCH_3 + H_2O \quad (3)$$

The separation performances of SOD membranes for equimolar mixtures of steam with H_2, CO_2, MeOH, DME or DMC, were evaluated in the temperature range from 125 to 200 °C. The mixture separation factors for steam from DME and DMC through the SOD membrane were found to be higher than 200 and 1000, respectively. To increase the hydrothermal stability of SOD membranes, SOD can be doped with sulfur.[263]

MFI membranes modified by catalytic cracking deposition (CCD) have been successfully evaluated in catalytic high-temperature water-gas shift (WGS) reactors.[264] Despite the relatively modest hydrogen selectivities ($\alpha_{H_2/CO_2} \approx 31$, $\alpha_{H_2/CO} \approx 25$), the CO conversion could be increased over the thermodynamic limit. MFI membranes modified by CCD coking have also been successfully evaluated in a low-temperature WGS reaction to overcome the equilibrium constraints (Fig. 11).[265]

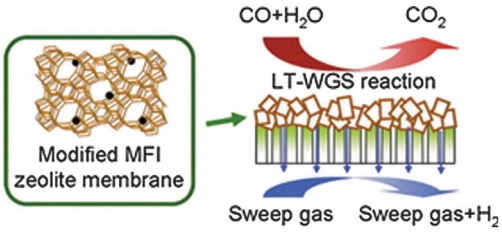

Fig. 11 Schema of a membrane supported water-gas shift reaction: In an extractor-type membrane reactor, hydrogen is selectively removed through an MFI membrane modified by coking. Reprinted from Y. Zhang, Z. Wu, Z. Hong, X. Gu and N. Xu, *Chem. Engin. J.*, 2012, **197**, 314–321 (ref. 265). Copyright 2012, with permission from Elsevier.

For the applications mentioned above, long term thermal and hydrothermal stability are important and they are addressed next.

11. Hydrothermal stability of zeolite membranes

Water vapor at temperatures higher than ~200 °C is present in many industrially important reactions (*e.g.* water gas shift (WGS), steam methane reforming (SMR), methanol synthesis, Fischer–Tropsch (FT)). This makes steam stability of membranes of immense importance for the realization of membranes in the chemical industry. Research in this area has primarily been focused on the effect of steam on catalytic activity of zeolites for use in catalysis. In general, steaming can cause dealumination *via* hydrolysis of Si–O–Al bonds and the formation of extra-framework aluminum oxide or hydroxide species.[266]

While these studies can provide some insights for the initial screening of zeolites for use in membrane fabrication, the concept of steam stability in membrane science requires different standards. Furthermore, all-silica zeolites, being intrinsically hydrophobic but not very active catalytically, are of particular interest for membrane studies in steam-containing environments. In this context, detailed short- and long-term steaming effect on the structure, morphology, film–support interaction, and grain boundaries need to be addressed. In practice, the effect of steam on membranes rather than powders can serve as a low-cost bullet proof test of membrane applicability for the intended process. In this section, we briefly cover the steam stability of zeolites followed by permeation studies in zeolite membranes involving high temperature steam.

Steaming of zeolite Y has been widely used to form an ultrastable Y (USY) catalyst for the petroleum industry. Stability comes from partial dealumination of the aluminum framework and incorporation of silica, by migration from other parts, into the generated vacancies.[267]

Kennedy *et al.*[268,269] and Ma *et al.*[270] studied the effect of water vapor on MCM-22 at 850 °C for 8 h and 450 and 550 °C for 2 h, respectively. Both found that steaming enhanced the spectral resolution of ^{29}Si solid state MAS NMR, pointing to the reduction of defects in the framework. It has been suggested that a minimum lifetime of 2–3 years is required for membranes to keep up with periodic turnarounds for maintenance in industry.[271]

Recently, the long-term steam stability of MWW framework zeolites (MCM-22 with Si/Al = 40 and all-silica ITQ-1) was investigated.[272] MCM-22, ITQ-1, and $SiCl_4$-treated ITQ-1 were steamed (95 mol% H_2O, 5 mol% N_2) at temperatures of 350 °C and 600 °C under 10 barg pressure for 84 days. At a high steaming temperature of 600 °C, both zeolites underwent significant morphological changes exhibiting cavity formation in the crystals and significant loss of microporosity. However, at a lower steaming temperature of 350 °C, MCM-22 and $SiCl_4$-treated ITQ-1 retained 70% and 60% of microporosity, respectively. Consistent with the studies of Ma *et al.* and Kennedy *et al.*, steaming enhanced the short range ordering of the crystals by reducing the structural defects (see Fig. 12). It was also found that defects in the structure can significantly lower the steam stability of zeolites. It was concluded that any efforts for application of zeolite membranes under such steaming conditions require eliminating (or minimizing) the structural defects. This can be achieved by methods such as fluoride synthesis or post-synthesis techniques ($SiCl_4$ treatment).[272]

In the following, some membrane permeation studies under water vapor at high temperatures are highlighted. While some of these reports are not directly aimed at investigating the long-term steam stability of membranes, they can provide valuable insights into the performance of difference zeolite membranes under steam conditions.

Sato *et al.*[273] investigated the performance of FAU-type zeolite membranes for application in methanol synthesis. It was shown that FAU-membranes can separate water and methanol from water–methanol–hydrogen mixtures at temperatures and pressures as high as 180 °C and 5 MPa, respectively. The authors attributed membrane selectivity to the preferential adsorption of water and methanol onto the zeolite.

Sawamura *et al.*[274] investigated the performance of mordenite membranes for water–methanol–hydrogen vapor mixtures in the temperature range of 150–250 °C and pressures up to 0.7 MPa. The water permeance was 1.8×10^{-8} mol m^{-2} s^{-1} Pa^{-1} while the separation factors for H_2O/H_2 and H_2O/CH_3OH at 250 °C were 50 and 75, respectively. In the absence of water in the feed, membranes lost their selectivity. The authors speculated that the zeolite water loss, in the absence of water in the feed at temperatures higher than 230 °C, caused the membrane failure by crack formation.

Sadat Rezai *et al.*[275] investigated the performance of MFI zeolite (silicalite-1 and ZSM-5) membranes in a ternary H_2O–H_2–*n*-hexane (in balance He) vapor mixture in the temperature range of 25–350 °C and at atmospheric pressure. Membranes showed the highest H_2O/H_2 separation factors of 15 and 20 at 25 °C for silicalite-1 and ZSM-5, respectively. However, at temperatures higher than 180 °C the separation factor approached 1. The loss of selectivity was attributed to the reduced water adsorption at higher temperatures. No negative effect of water on the zeolite structure or zeolite membrane integrity was reported in this study.

Masuda *et al.*[276] proposed catalytic cracking of silanes (CCS) to reduce the effective pore size of MFI zeolites. The idea was to deposit silanes inside the pores (as opposed to outside as a film) for separating small molecules for which MFI zeolites are otherwise not very selective (see Section 7). Highly hydrogen permselective MFI membranes were made at the cost of one order of magnitude reduction in permeance. Dong's group extensively studied[277] and enhanced this method by developing an on-stream catalytic cracking deposition (CCD) process using

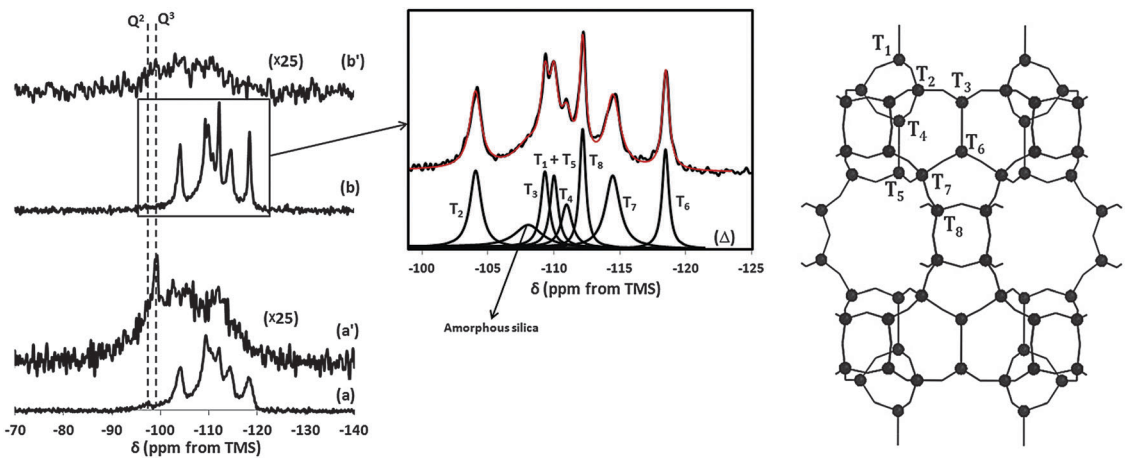

Fig. 12 ^{29}Si MAS NMR (a, b) and CP/MAS NMR (a′ and b′) spectra of MCM-22 (left): before (bottom) and after (top) 84 days of steaming at 350 °C and 10 barg (95% H_2O, 5% N_2), respectively. (Δ) is the deconvoluted components of the experimental spectrum (b) and the resulting fit is shown in the solid red line. Projection of the MWW unit cell viewed along the b axis with eight crystallographically unequivalent tetrahedral sites is shown on the right side. Reprinted from B. Elyassi, X. Zhang and M. Tsapatsis, *Microporous Mesoporous Mater.*, 2014, **193**, 134–144 (ref. 272). Copyright 2012, with permission from Elsevier.

methyldiethoxysilane (MDES). The modified MFI membranes were hydrogen permselective (H_2/CO_2 ideal selectivity as high as 19 and H_2 permeance of 1.5×10^{-7} mol m^{-2} s^{-1} Pa^{-1}) in the temperature range of 400–550 °C. Further, the membranes remained selective, although there was some loss in permeance and selectivity, under water gas shift reaction conditions after 1800 h (1100 h wet + 700 h dry) of testing.

Bernal *et al.*[278] investigated the effect of water vapor on the performance of ZSM-5 and composite mordenite/ZSM-5/chabazite membranes in the temperature range of 30–225 °C at atmospheric pressure. The ZSM-5 membrane was stable for ~60 h of testing under about 4 kPa of water vapor.

Lin's group[279] investigated ZSM-5 and silicalite-1 membranes under dry and wet mixture of H_2–CO_2 in the temperature range of 400–550 °C and pressures up to 388 kPa. They showed that water can have a suppression effect on the permeance of both hydrogen and carbon dioxide at these high temperatures. This effect was attributed to the intrinsic hydrophilicity of ZSM-5 and silanol groups in silicalite-1. The membranes showed a low H_2/CO_2 selectivity of about 3.5, however, no crack formation was reported.

Günther *et al.*[263] reported hydrothermally stable S-SOD (sulfur-doped sodalite) membranes for H_2/CO_2 separation. They indicated that S-SOD is stable at 270 °C and 40 bar in the presence of 30 wt% water.

It follows from the above that zeolites are not the thermodynamically most stable product. They can re-crystallize into dense phases or even become amorphous, but the energy barrier of these transformations is relatively high in comparison with MOFs. For MOFs, stability is a major issue. As an example, MOF-5 decomposes at room temperature in atmospheric air by hydrolysis. In some recent reviews by Canivet and Burtch, the limits and promises of the MOF stability towards water are treated.[280,281] In a previous pioneering paper by Low, a good overview of the steam stability of MOFs as a function of temperature is given.[282] In many studies on steam stability of MOF membranes, the tests have been carried out only for short periods of time (1–2 days) and it is hard to make conclusions on the long-term stability.[283,284]

12. Zeolite *vs.* MOF membranes – conceptual similarities and practical differences

Since certain MOFs show a permanent porosity and a reasonable stability such as the MOF subfamily of zeolitic imidazolate frameworks (ZIFs), the potential application fields of MOFs are similar to the applications of zeolites. These include gas storage, separation by adsorption and heterogeneous catalysis. Consequently, MOFs have also been evaluated as a supported μm-sized membrane layer in gas separation, as highlighted in a recent review by Qiu *et al.*[137] Due to the similarity of MOFs and zeolites[285] (Table 1), in a relatively short time interval, supported MOF membranes could be synthesized successfully by using the whole tool box developed for the preparation of supported zeolite membranes: seeding of macroporous ceramics, microwave heating and of surface charges (zeta potential) and covalent bonds between ceramic support and MOF layer. On the other hand, the differences between zeolites and MOFs are also addressed in Table 1.

In the following, (i) synthesis and (ii) molecular sieving of zeolite and MOF membranes will be compared.

While most zeolite membranes are synthesized under hydrothermal conditions in autoclaves at $T > 100$ °C, MOF membranes can be prepared at room temperature. Furthermore, most zeolite membranes are synthesized by means of a structure-directing agent (SDA, also called template), which is incorporated into the zeolite framework during synthesis and cannot be easily removed by desorption or extraction because of its bulkiness. Therefore, zeolite membranes usually require a thermal activation by combusting the organic SDA. In contrast, occluded solvent molecules can be easily removed from MOFs, which allows the formation of coatings on thermally sensitive materials like polymers. In the last few years several low-temperature synthesis methods for MOF layers on organic substrates have been developed which have no counterpart in the field of zeolites.

Some commonly used approaches for MOF thin film preparation are growth from solvothermal mother solutions (using self-assembled monolayers or SAMS),[290–292] colloidal deposition, layer-by-layer or liquid phase epitaxy of SURMOFs,[293–297] electrochemical synthesis,[298–301] evaporation induced crystallization, gel-layer synthesis and microwave-induced thermal deposition.[302,303]

If a porous support is used for the separation of an aqueous and an organic solvent, one of the solvents contains the metal ion and the other contains the linker molecule. A MOF layer forms at the contact zone of the polymer support–aqueous solvent[304,305] or inorganic support–organic solvent.[306] Recently, a concept for a scalable and inexpensive processing of MOF membranes in polymeric hollow fibers has been developed.[117]

In the layer-by-layer deposition technique,[307] a support is repeatedly dipped into a solvent containing metal ions or linker molecules with a washing step in between. A severe difference between zeolite and MOF membranes is their different molecular sieve behaviour. Whereas perfect zeolite membranes show very high separation selectivities due to molecular sieving, MOF membranes show no sharp cut-off. As examples for molecular sieving on zeolite membranes, three highlights are given: (i) xylene isomer separation on MFI membranes with mixed gas selectivities of >500,[308] (ii) CO_2/CH_4 separation on SAPO-34 membranes with a selectivity >100[224], and (iii) CO_2/CH_4 separation on DDR membranes with a selectivity 300–600.[226] These selectivities are mainly based on molecular sieving with a fixed pore size. By using efficient computational methods, the pore size of >250 000 hypothetical silica zeolites has been characterized[214] providing information on the largest molecule that can permeate through or adsorb in each zeolite membrane. The library of the >250 000 hypothetical silica zeolites has been generated by Deem *et al.*[309]

In many cases, due to poor membrane–substrate bonding, it remains difficult to prepare continuous MOFs by this method.

Table 1 Comparison of the main properties of zeolites and MOFs

Metal–organic frameworks (MOFs)	Zeolites
Metal or metal oxide cluster cations interconnected by organic anions with permanent porosity after solvent removal.[286] Coordination polymers with comparatively strong ionic-covalent bonds (coordinative bonds). Rather flexible framework, often structure change after solvent removal (''breathing''), therefore MOFs are called ''soft porous crystals''.	Microporous aluminosilicates with counterions, also cation-free silicates, aluminum phosphates *etc.* Porous metal oxide structure with high contribution of covalent bonds, yielding a rigid framework.
Often MOFs possess a dynamic framework due to effects like bond angle and cluster deformation and/or linker twisting/rotation. These effects result in a flexible pore size for guest molecules with no clear ''cut off'' in molecular sieving and ''gate opening'' (guest incorporation becomes possible at a threshold pressure).	Relatively fixed pore size that allows molecular sieving with a clear ''cut off''. But also for zeolites, temperature or adsorption of guest molecules can induce structure changes. For ZSM-5 and other pentasils, a transition between monoclinic and orthorhombic framework forms is found with a change of temperature or the adsorption of ring-containing guest molecules.[287–289]
Activation by solvent removal (drying) at $T < 100\ ^{\circ}C$ and also solvent replacement. MOF layers on cheap polymer supports as membrane coating are possible.	In most cases, organic structure-directing agents (template) are incorporated into the structure. Activation is by calcination, which can cause damage to the zeolite structure.
Vulnerable towards humidity and temperature in most cases. Exceptions are some ZIFs (Zn/Co-imidazolates) and some carboxylate MOFs with high-valent cations (Zr^{4+}/Cr^{3+}) which show a high stability against decomposition. Porous MOFs are thermodynamically unstable and transformation into dense phases possible.	Rather stable in humidity and at high temperatures. Zeolites are not the thermodynamically most stable phase (quartz, cordierite, mullite), but transformation rate into dense structures is low due to a high activation barrier.
Design of pore opening and adsorptive interaction through a variety of functional groups on the organic linker molecule possible. Post synthetic modification and post synthetic linker exchange possible for membrane functionalization.	Less modifications possible, pore size is crystallographically controlled. Only in some cases, pore size engineering by counterion exchange is possible.
Certain MOF structures offer accessible open metal sites like Co, Mn, Fe in MOF-74 for (coordinative–adsorptive) interaction with guest such as olefins, carbon dioxide.	The framework T-atoms Al, Si or P are not accessible since they are surrounded and hidden by large oxygen ions. Also, counter cations not always accessible if they are on certain cation positions.
Great potential as a mixed matrix membrane.	Great potential as a supported thin-film membrane in dehydration and isomer separation.

A method of 'single metal source' has been developed to facilely prepare a homochiral MOF membrane on a nickel net, which played a dual role as the only nickel source added to the reaction system and as a substrate supporting the membrane.[310] Also, Nagaraju *et al.* demonstrated the synthesis of CuBTC on a polysulfone based porous asymmetric ultrafiltration (UF) membrane by *in situ* growth followed by the LBL deposition of crystals without any need for pre-seeding or surface modification of the membrane. In this way, the top surface of the UF membrane pores is completely covered by MOFs; while the remaining part of the membrane offers a flexible support to the MOFs.[311]

To improve membrane–substrate bonding, a self-assembled monolyer (SAM) can serve to chemically modify the supports to improve heterogeneous nucleation. Recently, Huang *et al.* reported a highly permeable and selective ZIF-95 membrane for H_2/CO_2 separation with the APTES-modified asymmetric α-Al_2O_3 disk.[312] Fan *et al.* treated a glass-frit disk with $(NH_4)_2SiF_6$ which was able to bind the membrane and the substrate by integrating F atoms in the substrate surface.[313] Ben *et al.* reported using a PMMA–PMAA coated stainless steel net to fabricate HKUST-1 intact free-standing MOF membranes.[314]

Besides the methods above, reactive seeding is another important method used in secondary growth to achieve a uniform, thin, well intergrown MOF membrane. In this method, the seed layer is produced by the reaction between the inorganic support and the organic precursor in a single stage. This method has been widely reported.[315–318]

There is also much progress in the prediction of pore size and functionalities of MOFs. In the so-called isoreticular chemistry,[319] desired topologies can be achieved by design and isoreticular series of compounds with the same topology but different pore sizes can be prepared.[320,321] However, most MOF membranes show no clear cut-off in gas adsorption and membrane permeation. As a coordination polymer they allow bond angle and cluster deformation and/or linker twisting/rotation. These effects result in a flexible pore size for guest molecules with no clear "cut off" in molecular sieving and "gate opening" (guest incorporation becomes possible at a threshold pressure).

As an example, for the MOF of type ZIF-8 (zeolitic imidazolate framework-8), the Zn^{2+} ions are interconnected by methylimidazolate ions.[322] The synthesis and permeation studies of ZIF-8 membranes have been widely reported.[306,323–326] There are some recent reports that the framework adsorbs bulky molecules such as benzene or xylenes,[327,328] despite its pore openings of 3.4 Å as found from Rietveld XRD analysis. Hence, it is possible that adsorbed molecules can "open the gate" under certain conditions,[329–337] as illustrated in Fig. 13.

Additionally, gas sorption studies on different ZIF powders show hysteresis that arises from threshold pressures which induce the "gate opening". In a recent theoretical paper,[338] Density Functional Theory (DFT) has been used to unravel the vibration patterns of selected ZIFs (ZIFs 4, 7 and 8) on a molecular level. Vibrations in the THz region can explain such cooperative phenomena of "gate opening" and "breathing"

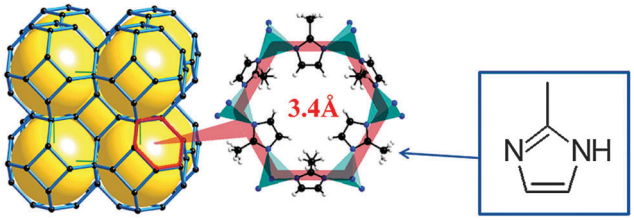

Fig. 13 Left: the SOD structure of ZIF-8. Middle: the Rietveld mechanism leads to a pore size of 3.4 Å of the 6-ring for molecules to become adsorbed by ZIF-8 or to pass a ZIF-8 membrane. However, by a thermally initiated flip-flop motion of the linker molecule methyl-imidazolate (right), the pore size can be much wider. Adapted from H. Bux, F. Liang, Y. Li, J. Cravillon, M. Wiebcke and J. Caro, *J. Am. Chem. Soc.*, 2009, **131**, 16000–16001 (ref. 337). Copyright 2009, with permission from the American Chemical Society.

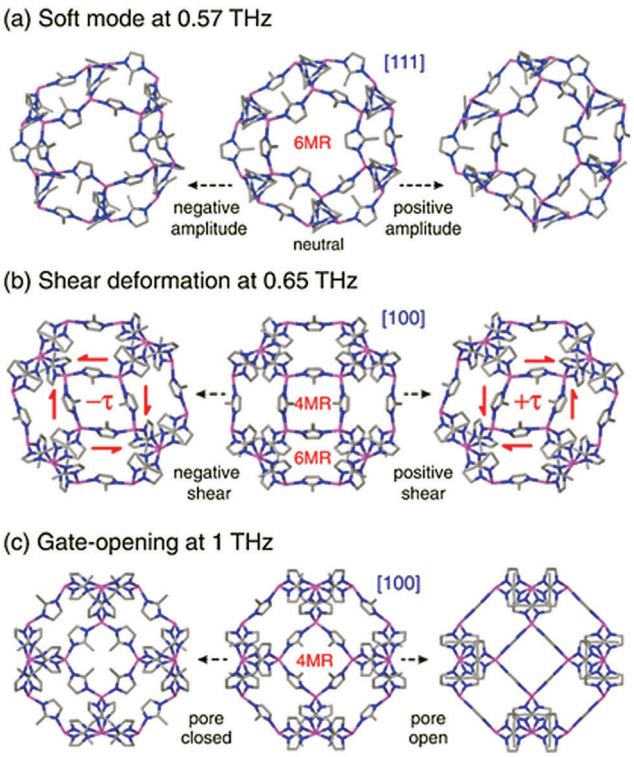

Fig. 14 Low-frequency lattice dynamics of a SOD cage of ZIF-8. Reprinted from ref. 338. Copyright 2014 by the American Physical Society.

(see Fig. 14). In other words, these DFT calculations support the assumptions of a flexible pore architecture and support the absence of a clear cut off as found in numerous permeation experiments on MOF membranes.

However, it is a fact that the effective pore size of MOFs as "soft porous crystals" can be controlled in a manner that is characteristic of molecular sieve materials. A case in point is the "mixed linker" concept which has been studied extensively for the ZIFs, demonstrating that by a fine control of the effective pore size, high selectivities can be obtained in separations. Thompson *et al.* showed that substitution of ZIF-7 linkers (benzimidazole) in a ZIF-8 framework (methylimidazolate linker) rigidifies the material.[339] Eum *et al.* showed the control of

butane isomer selectivities over 3 orders of magnitude by substitution of ZIF-8 linkers in ZIF-90.[340]

13. Mixed matrix membranes (MMMs) made of zeolites and MOFs

It is an old dream to have a μm-sized zeolite or a MOF layer as a gas selective membrane. However, such a supported molecular sieve membrane of a thin zeolite or a MOF layer on a mechanically strong porous ceramic or a metal support is difficult to prepare and to scale up. Therefore, the idea was born to combine the molecular sieving and adsorption properties of zeolites or MOFs with the excellent processing properties of polymers by mixing (nano) particles of a zeolite or MOF with a traditional polymer. For the membrane processing, established technologies such as hollow fiber spinning or foil casting are used to produce thin and mechanically stable membranes.

Whereas the progress with zeolite-based MMMs during the last 20 years was very limited – most probably the inorganic zeolite and the organic polymer do not match very well despite surface modification of the zeolite – there has been a considerable activity in revisiting this concept with MOF-based MMMs.

In several recent papers, an improved separation behavior of MMMs with nano-particulate fillers – as shown in Fig. 15 – is reported.[341–345] In principle, the lab-scale fabrication procedure of MOF-based MMMs is similar to the one applied for the synthesis of other MMMs. This involves the phase-inversion and solution-casting methods. Regarding the fillers, HKUST-1, ZIF-8 and MIL-50(Al) with and without amino groups have been the most studied MOFs. As for the polymers, the organic phase can be classified into low flux glassy polymers (*i.e.* PSF,[346–350] Ultem®,[351,352] Matrimid®[109–111,348,349,351,353–357] or PBI)[110,358] and high flux polymers: rubbery, such as PDMS[359] and glassy, such as 6FDA-DAM.[351]

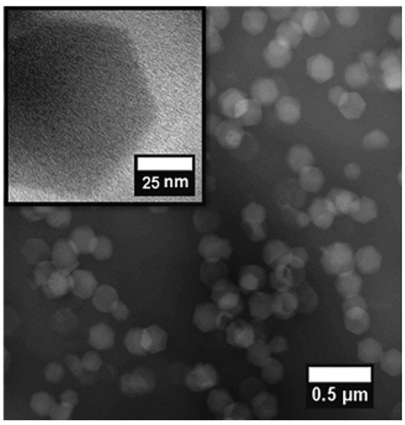

Fig. 15 STEM (inset) and TEM of a 25 vol% MOF-based ZIF-8/matrimid MMMs. Note that the ZIF-8 nanocrystals are homogenously distributed and well embedded in the matrimid matrix. Reprinted from L. Diestel, N. Wang, A. Schulz, F. Steinbach and J. Caro, *Ind. Eng. Chem. Res.*, 2015, **54**, 1103–1112 (ref. 372). Copyright 2015, with permission from the American Chemical Society.

In a large percentage of the reported results, improvements in flux at constant selectivities with respect to the bare polymer have been reported and only in circa 10% of the cases improvements in both flux and selectivity were achieved. Besides, for all the membranes tested at high pressures it was observed that upon MOF addition, the plasticization of the membrane at high CO_2 pressures was partially suppressed, maintaining large separation factors over a wider pressure range than that observed for the pure polymer[351,359] or even increasing the selectivity at high pressures.[360] For industrial application, besides reports based on asymmetric flat membranes,[361] the progress in hollow fiber membranes is primarily on ZIF-8 based membranes (see Section 6). Asymmetric MMMs of MOFs in different polymers have also been recently obtained.[362–365]

MMMs are most effective if nanosheets are incorporated into the polymer as shown schematically in Fig. 16. Some molecules go the short way through the membrane by passing the porous sheets; other molecules cannot since they are too bulky and therefore they have to go the long tortuosity way around the sheets through the neat polymer.

Just recently, two papers on the synthesis of MOF nanosheets for MOF membrane applications appeared: in both papers MOF nanosheets are prepared and used in mixed matrix or stacked sheet membranes as molecular sieves for gas separation. Rodenas *et al.* followed a bottom-up concept: MOF nanosheets are formed in the contact zone of a linker and a metal solution followed by sedimentation.[110] In contrast, Peng *et al.* have used a top-down strategy: a two-dimensional MOF is exfoliated by first wet ball-milling followed by exfoliation in a solvent under ultra-sonication.[62] These studies on MOF

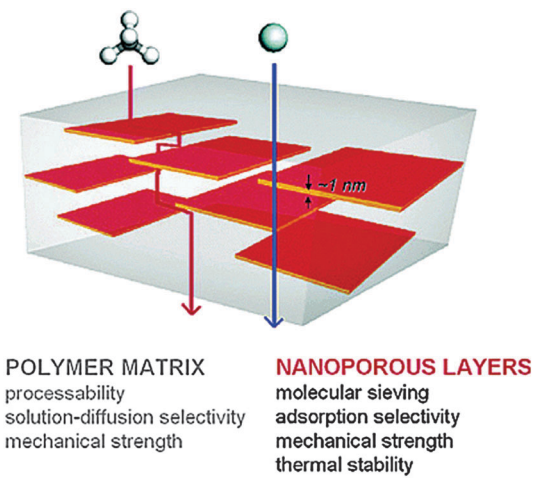

Fig. 16 The concept of membranes containing selective flakes embedded in a matrix was introduced in 1990 by Cussler (ref. 112) and later modified with the idea of including nanometer-thick nanoporous layers (ref. 366 and 373) instead of plate-like crystals. Despite progress with silicate, aluminophosphate, MOF and graphene layers, this concept has not yet been realized fully, *i.e.*, with completely exfoliated crystalline nanoporous layers and proof that the layers preserved their pore structure upon exfoliation and incorporation in the matrix. Reprinted from H.-K. Jeong, W. Krych, H. Ramanan, S. Nair, E. Marand and M. Tsapatsis, *Chem. Mater.*, 2004, **16**, 3838–3845 (ref. 373). Copyright 2004, with permission from the American Chemical Society.

nanosheets draw on earlier concepts of making dispersible exfoliated zeolite nanosheets to apply them as a selective membrane.[23,25,366–368] The same concept is followed when graphene oxide sheets are stacked and form a thin gas selective layer.[61,369] By the sophisticated processing technology, a brick-layer structure of the MOF sheets is formed which is crucial for gas transport through a polymer membrane containing selectively permeable flakes as for the first time proposed in ref. 112 and further analyzed in ref. 370 and 371

14. Outlook and perspectives

Within the next 5 years, further capacities will be installed for the drying of organic liquids such as ethanol, acetonitrile, glycerol *etc.* by steam permeation/pervaporation using LTA membranes. However, despite much progress in the development of supported thin-layer zeolite membranes, there is still no gas separation using zeolite membranes in industrial use.

The relatively high costs of the supported zeolite membranes are due to the asymmetric graded ceramic multi-layer support. Extrusion of multi-channel monoliths or the use of temperature-stable hollow fiber polymer supports can be proper solutions.

The scale up of supported zeolite and MOF membranes will remain a challenge (discontinuous autoclave technology). Membrane formation by processes amenable to continuous processing (*e.g.* extrusion, spinning, coating-based) should be the technological focus. Well characterized membrane microstructures (*e.g.* preferred orientation, designed interfaces, grain boundary control), emphasis on reproducibility and stability of performance under multicomponent mixtures should remain the focus of fundamental studies.

Acknowledgements

JC thanks Xuehong Gu, Nanjing University of Technology and Jiangsu Nine Heaven High-Tech Co. Ltd as well as Yanshuo Li and Weisen Yang, Dalian Institute of Chemical Physics, for information on the technical application of LTA membranes in solvent dehydration. Stefan Kaskel (TU Dresden), Sankar Nair (Georgia Tech) and Michael Wiebcke (Leibniz University Hannover) are thanked for stimulating discussions.

Notes and references

1 J. Gascon, F. Kapteijn, B. Zornoza, V. Sebastián, C. Casado and J. Coronas, *Chem. Mater.*, 2012, **24**, 2829–2844.
2 S. R. Venna and M. A. Carreon, *Chem. Eng. Sci.*, 2015, **124**, 3–19.
3 B. Seoane, J. Coronas, I. Gascon, M. E. Benavides, O. Karvan, J. Caro, F. Kapteijn and J. Gascon, *Chem. Soc. Rev.*, 2015, **44**, 2421–2454.
4 H. B. Tanh Jeazet, C. Staudt and C. Janiak, *Dalton Trans.*, 2012, **41**, 14003–14027.
5 T. C. T. Pham, H. S. Kim and K. B. Yoon, *Science*, 2011, **334**, 1533–1538.
6 N. Rangnekar, M. Shete, K. V. Agrawal, B. Topuz, P. Kumar, Q. Guo, I. Ismail, A. Alyoubi, S. Basahel, K. Narasimharao, C. W. Macosko, K. A. Mkhoyan, S. Al-Thabaiti, B. Stottrup and M. Tsapatsis, *Angew. Chem., Int. Ed.*, 2015, **54**, 6571–6575.
7 T. C. T. Pham, T. H. Nguyen and K. B. Yoon, *Angew. Chem., Int. Ed.*, 2013, **52**, 8693–8698.
8 Y. Peng, H. Lu, Z. Wang and Y. Yan, *J. Mater. Chem. A*, 2014, **2**, 16093–16100.
9 D. Korelskiy, T. Leppäjärvi, H. Zhou, M. Grahn, J. Tanskanen and J. Hedlund, *J. Membr. Sci.*, 2013, **427**, 381–389.
10 K. V. Agrawal, B. Topuz, Z. Jiang, K. Nguenkam, B. Elyassi, M. Navarro, L. F. Francis and M. Tsapatsis, *AIChE J.*, 2013, **59**, 3458–3467.
11 K. V. Agrawal, B. Topuz, T. C. T. Pham, T. H. Nguyen, N. Sauer, N. Rangnekar, H. Zhang, K. Narasimharao, S. Basahel, L. F. Francis, C. W. Macosko, S. Al-Thabaiti, M. Tsapatsis and K. B. Yoon, *Adv. Mater.*, 2015, **27**, 3243–3249.
12 M. Tsapatsis, *Science*, 2011, **334**, 767–768.
13 S. Mintova, J.-P. Gilson and V. Valtchev, *Nanoscale*, 2013, **5**, 6693–6703.
14 G. Bonilla, I. Diaz, M. Tsapatsis, H. Jeong, Y. Lee and D. G. Vlachos, *Chem. Mater.*, 2004, **382**, 5697–5705.
15 G. N. Karanikolos, J. W. Wydra, J. A. Stoeger, H. Garcia, A. Corma and M. Tsapatsis, *Chem. Mater.*, 2007, **19**, 792–797.
16 H. Awala, J.-P. Gilson, R. Retoux, P. Boullay, J.-M. Goupil, V. Valtchev and S. Mintova, *Nat. Mater.*, 2015, 1–5.
17 M. A. Snyder and M. Tsapatsis, *Angew. Chem., Int. Ed.*, 2007, **46**, 7560–7573.
18 W. Fan, M. a. Snyder, S. Kumar, P.-S. Lee, W. C. Yoo, A. V. McCormick, R. Lee Penn, A. Stein and M. Tsapatsis, *Nat. Mater.*, 2008, **7**, 984–991.
19 P. Lee, X. Zhang, J. A. Stoeger, A. Malek, W. Fan, S. Kumar, W. C. Yoo, S. Al Hashimi, R. L. Penn, A. Stein and M. Tsapatsis, *J. Am. Chem. Soc.*, 2011, **133**, 493–502.
20 H. Chen, J. Wydra, X. Zhang, P. S. Lee, Z. Wang, W. Fan and M. Tsapatsis, *J. Am. Chem. Soc.*, 2011, **133**, 12390–12393.
21 W. J. Roth, P. Nachtigall, R. E. Morris and J. Čejka, *Chem. Rev.*, 2014, **114**, 4807–4837.
22 U. Díaz and A. Corma, *Dalton Trans.*, 2014, **43**, 10292–10316.
23 M. Tsapatsis, *AIChE J.*, 2014, **60**, 2374–2381.
24 A. Corma, V. Fornes, S. B. Pergher, T. L. M. Maesan and J. G. Buglass, *Nature*, 1998, **396**, 353–356.
25 K. V. Agrawal, X. Zhang, B. Elyassi, D. D. Brewer, M. Gettel, S. Kumar, J. A. Lee, S. Maheshwari, A. Mittal, C.-Y. Sung, M. Cococcioni, L. F. Francis, A. V. McCormick, K. A. Mkhoyan and M. Tsapatsis, *Science*, 2011, **334**, 72–75.
26 K. B. Yoon, *Acc. Chem. Res.*, 2007, **40**, 29–40.
27 Y. S. Chun, K. Ha, Y.-J. Lee, J. S. Lee, H. S. Kim, Y. S. Park and K. B. Yoon, *Chem. Commun.*, 2002, 1846–1847.

28 A. Huang and J. Caro, *J. Mater. Chem.*, 2011, **21**, 11424.
29 A. Huang, F. Liang, F. Steinbach and J. Caro, *J. Membr. Sci.*, 2010, **350**, 5–9.
30 A. Huang and J. Caro, *Chem. Mater.*, 2010, **22**, 4353–4355.
31 Y. Peng, Z. Zhan, L. Shan, X. Li, Z. Wang and Y. Yan, *J. Membr. Sci.*, 2013, **444**, 60–69.
32 B. Zhu, D. T. Myat, J.-W. Shin, Y.-H. Na, I.-S. Moon, G. Connor, S. Maeda, G. Morris, S. Gray and M. Duke, *J. Membr. Sci.*, 2015, **475**, 167–174.
33 W. C. Yoo, J. a Stoeger, P.-S. Lee, M. Tsapatsis and A. Stein, *Angew. Chem., Int. Ed.*, 2010, **49**, 8699–8703.
34 E. Hu, Y. L. W. Huang, Q. Yan, D. Liu and Z. Lai, *Microporous Mesoporous Mater.*, 2009, **126**, 81–86.
35 C. Wang, X. Liu, J. Li and B. Zhang, *CrystEngComm*, 2013, **15**, 6301–6304.
36 M. Zhou, D. Korelskiy, P. Ye, M. Grahn and J. Hedlund, *Angew. Chem., Int. Ed.*, 2014, **53**, 3492–3495.
37 X. Shu, X. Wang, Q. Kong, X. Gu and N. Xu, *Ind. Eng. Chem. Res.*, 2012, **51**, 12073–12080.
38 M. Zhou, M. Grahn, H. Zhou, A. Holmgren and J. Hedlund, *Chem. Commun.*, 2014, **50**, 14261–14264.
39 J. S. Lee, K. Ha, Y. J. Lee and K. B. Yoon, *Adv. Mater.*, 2005, **17**, 837–841.
40 K. B. Blodgett, *J. Am. Chem. Soc.*, 1934, **56**, 495.
41 I. Langmuir and V. J. Schaefer, *J. Am. Chem. Soc.*, 1938, **60**, 1351–1360.
42 M. C. Petty, *Langmuir–Blodgett Films An Introduction*, Cambridge University Press, 1996.
43 L. Imperiali, K. Liao, C. Clasen, J. Fransaer, C. W. Macosko and J. Vermant, *Langmuir*, 2012, **28**, 7990–8000.
44 K. Ariga, Y. Yamauchi, T. Mori and J. P. Hill, *Adv. Mater.*, 2013, **25**, 6477–6512.
45 K. Morawetz, J. Reiche, H. Kamusewitz, H. Kosmella and R. Ries, *Colloids Surf., A*, 2002, **200**, 409–414.
46 Z. Wang, L. H. Wee, B. Mihailova, K. J. Edler and A. M. Doyle, *Chem. Mater.*, 2007, **19**, 5806–5808.
47 L. Tosheva, V. P. Valtchev, B. Mihailova and A. M. Doyle, *J. Phys. Chem. C*, 2007, **111**, 12052–12057.
48 L. H. Wee, Z. Wang, L. Tosheva, L. Itani, V. Valtchev and A. M. Doyle, *Microporous Mesoporous Mater.*, 2008, **116**, 22–27.
49 Z. Wang, T. Yu, P. Nian, Q. Zhang, J. Yao, S. Li, Z. Gao and X. Yue, *Langmuir*, 2014, **30**, 4531–4534.
50 J. Li, X. Liu, X. Lv and B. Zhang, *Mater. Lett.*, 2014, **124**, 299–301.
51 R. Makiura, S. Motoyama, Y. Umemura, H. Yamanaka, O. Sakata and H. Kitagawa, *Nat. Mater.*, 2010, **9**, 565–571.
52 R. Makiura and O. Konovalov, *Nature*, 2013, **3**, 1–8.
53 S. Motoyama, R. Makiura, O. Sakata and H. Kitagawa, *J. Am. Chem. Soc.*, 2011, **133**, 5640–5643.
54 W. Wang, X. Dong, J. Nan, W. Jin, Z. Hu, Y. Chen and J. Jiang, *Chem. Commun.*, 2012, **48**, 7022–7024.
55 D.-J. Lee, Q. Li, H. Kim and K. Lee, *Microporous Mesoporous Mater.*, 2012, **163**, 169–177.
56 B. Liu, O. Shekhah, H. K. Arslan, J. Liu, C. Woll and R. A. Fischer, *Angew. Chem., Int. Ed.*, 2012, **51**, 807–810.
57 A. Bétard, H. Bux, S. Henke, D. Zacher, J. Caro and R. A. Fischer, *Microporous Mesoporous Mater.*, 2012, **150**, 76–82.
58 J. Benito, M. Fenero, S. Sorribas, B. Zornoza, K. J. Msayib, N. B. McKeown, C. Téllez, J. Coronas and I. Gascón, *Colloids Surf., A*, 2015, **470**, 161–170.
59 X. Chen, J. Wang, D. Yin, J. Yang, J. Lu, Y. Zhang and Z. Chen, *AIChE J.*, 2013, **59**, 936–947.
60 H. Li, J. Wang, J. Xu, X. Meng, B. Xu, J. Yang, S. Li, J. Lu, Y. Zhang, X. He and D. Yin, *J. Membr. Sci.*, 2013, **444**, 513–522.
61 H. Li, Z. Song, X. Zhang, Y. Huang, S. Li, Y. Mao, H. J. Ploehn, Y. Bao and M. Yu, *Science*, 2013, **342**, 95–98.
62 Y. Peng, Y. Li, Y. Ban, H. Jin, W. Jiao, X. Liu and W. Yang, *Science*, 2014, **346**, 1356–1359.
63 W. Chaikittisilp, M. E. Davis and T. Okubo, *Chem. Mater.*, 2007, **19**, 4120–4122.
64 J. S. Lee, J. H. Kim, Y. J. Lee, N. C. Jeong and K. B. Yoon, *Angew. Chem., Int. Ed.*, 2007, **46**, 3087–3090.
65 X. Li, Y. Peng, Z. Wang and Y. Yan, *CrystEngComm*, 2011, **13**, 3657–3660.
66 X. Li, Y. Yan and Z. Wang, *Ind. Eng. Chem. Res.*, 2010, **49**, 5933–5938.
67 Y. Liu, Y. Li, R. Cai and W. Yang, *Chem. Commun.*, 2012, **48**, 6782–6784.
68 A. I. Lupulescu and J. D. Rimer, *Science*, 2014, **344**, 729–732.
69 H. F. Greer, *Mater. Sci. Technol.*, 2014, **30**, 611–626.
70 M. L. Gualtieri, *Microporous Mesoporous Mater.*, 2009, **117**, 508–510.
71 Y. Peng, X. Lu, Z. Wang and Y. Yan, *Angew. Chem., Int. Ed.*, 2015, **54**, 1–5.
72 M. E. Davis, *Chem. Mater.*, 2014, **26**, 239–245.
73 K. Iyoki, K. Itabashi and T. Okubo, *Microporous Mesoporous Mater.*, 2014, **189**, 22–30.
74 K. Itabashi, Y. Kamimura, K. Iyoki, A. Shimojima and T. Okubo, *J. Am. Chem. Soc.*, 2012, **134**, 11542–11549.
75 M. D. Oleksiak and J. D. Rimer, *Rev. Chem. Eng.*, 2014, **30**, 1–49.
76 B. Xie, J. Song, L. Ren, Y. Ji, J. Li and F.-S. Xiao, *Chem. Mater.*, 2008, **20**, 4533–4535.
77 B. Xie, H. Zhang, C. Yang, S. Liu, L. Ren, L. Zhang, X. Meng, B. Yilmaz, U. Müller and F.-S. Xiao, *Chem. Commun.*, 2011, **47**, 3945–3947.
78 Y. Kamimura, S. Tanahashi, K. Itabashi, A. Sugawara, T. Wakihara, A. Shimojima and T. Okubo, *J. Phys. Chem. C*, 2011, **115**, 744–750.
79 K. Honda, A. Yashiki, M. Itakura, Y. Ide, M. Sadakane and T. Sano, *Microporous Mesoporous Mater.*, 2011, **142**, 161–167.
80 K. Iyoki, K. Itabashi and T. Okubo, *Chem. – Asian J.*, 2013, **8**, 1419–1427.
81 G. Wu, W. Wu, X. Wang, W. Zan, W. Wang and C. Li, *Microporous Mesoporous Mater.*, 2013, **180**, 187–195.
82 Q. Wu, X. Wang, G. Qi, Q. Guo, S. Pan, X. Meng, J. Xu, F. Deng, F. Fan, Z. Feng, C. Li, S. Maurer, U. Mu and F. Xiao, *J. Am. Chem. Soc.*, 2014, **136**, 4019–4025.

83 G. Majano, A. Darwiche, S. Mintova and V. Valtchev, *Ind. Eng. Chem. Res.*, 2009, **48**, 7084–7091.
84 H. Zhang, C. Yang, L. Zhu, X. Meng, B. Yilmaz, U. Müller, M. Feyen and F.-S. Xiao, *Microporous Mesoporous Mater.*, 2012, **155**, 1–7.
85 A. Yashiki, K. Honda, A. Fujimoto, S. Shibata, Y. Ide, M. Sadakane and T. Sano, *J. Cryst. Growth*, 2011, **325**, 96–100.
86 E. Ng, J. Goupil, C. Fernandez, R. Retoux, V. Valtchev and S. Mintova, *Chem. Mater.*, 2012, **24**, 4758–4765.
87 Z. Tang, S. J. Kim, X. Gu and J. Dong, *Microporous Mesoporous Mater.*, 2009, **118**, 224–231.
88 H. Wang and Y. S. Lin, *J. Membr. Sci.*, 2012, **396**, 128–137.
89 M.-H. Zhu, Z.-H. Lu, I. Kumakiri, K. Tanaka, X.-S. Chen and H. Kita, *J. Membr. Sci.*, 2012, **415–416**, 57–65.
90 Y. Tang, X. Liu, S. Nai and B. Zhang, *Chem. Commun.*, 2014, **50**, 8834–8837.
91 E. Sjöberg, L. Sandström, O. G. W. Öhrman and J. Hedlund, *J. Membr. Sci.*, 2013, **443**, 131–137.
92 J. Hedlund, J. Sterte, M. Anthonis, A. Bons, B. Carstensen, N. Corcoran, D. Cox, H. Deckman, W. De Gijnst, P. De Moor, F. Lai, J. Mchenry, W. Mortier, J. Reinoso and J. Peters, *Microporous Mesoporous Mater.*, 2002, **52**, 179–189.
93 H. Zhou, D. Korelskiy, E. Sjöberg and J. Hedlund, *Microporous Mesoporous Mater.*, 2014, **192**, 76–81.
94 H. H. Funke, B. Tokay, R. Zhou, E. W. Ping, Y. Zhang, J. L. Falconer and R. D. Noble, *J. Membr. Sci.*, 2012, **409–410**, 212–221.
95 I. Kumakiri, M. Stange, T. a. Peters, H. Klette, H. Kita and R. Bredesen, *Microporous Mesoporous Mater.*, 2008, **115**, 33–39.
96 I. Tiscornia, I. Kumakiri, R. Bredesen, C. Télleza and J. Coronas, *Sep. Purif. Technol.*, 2010, **73**, 8–12.
97 R. Zhou, E. W. Ping, H. H. Funke, J. L. Falconer and R. D. Noble, *J. Membr. Sci.*, 2013, **444**, 384–393.
98 H. H. Funke, M. Z. Chen, A. N. Prakash, J. L. Falconer and R. D. Noble, *J. Membr. Sci.*, 2014, **456**, 185–191.
99 N. Peng, N. Widjojo, P. Sukitpaneenit, M. M. Teoh, G. G. Lipscomb, T. S. Chung and J. Y. Lai, *Prog. Polym. Sci.*, 2012, **37**, 1401–1424.
100 D. Q. Vu, W. J. Koros and S. J. Miller, *J. Membr. Sci.*, 2003, **211**, 311–334.
101 R. Mahajan and W. J. Koros, *Ind. Eng. Chem. Res.*, 2000, **39**, 2692–2696.
102 C. M. Zimmerman, A. Singh and W. J. Koros, *J. Membr. Sci.*, 1997, **137**, 145–154.
103 M. G. Süer, N. Baç and L. Yilmaz, *J. Membr. Sci.*, 1994, **91**, 77–86.
104 P. Sukitpaneenit, T. S. Chung and L. Y. Jiang, *J. Membr. Sci.*, 2010, **362**, 393–406.
105 T. S. Chung, L. Y. Jiang, Y. Li and S. Kulprathipanja, *Prog. Polym. Sci.*, 2007, **32**, 483–507.
106 T. T. Moore and W. J. Koros, *J. Mol. Struct.*, 2005, **739**, 87–98.
107 R. Patel, J. T. Park, H. P. Hong, J. H. Kim and B. R. Min, *Polym. Adv. Technol.*, 2011, **22**, 768–772.
108 I. Kiesow, D. Marczewski, L. Reinhardt, M. Mu, M. Possiwan and W. A. Goedel, *J. Am. Chem. Soc.*, 2013, **135**, 4380–4388.
109 C. J. Duan, X. M. Jie, D. D. Liu, Y. M. Cao and Q. Yuan, *J. Membr. Sci.*, 2014, **466**, 92–102.
110 T. Rodenas, I. Luz, G. Prieto, B. Seoane, H. Miro, A. Corma, F. Kapteijn, F. L. i Xamena and J. Gascon, *Nat. Mater.*, 2015, **14**, 48–55.
111 S. Sorribas, A. Kudasheva, E. Almendro, B. Zornoza, Ó. de la Iglesia, C. Téllez and J. Coronas, *Chem. Eng. Sci.*, 2015, **124**, 37–44.
112 E. L. Cussler, *J. Membr. Sci.*, 1990, **52**, 275–288.
113 J. Li, J. Shao, Q. Ge, G. Wang, Z. Wang and Y. Yan, *Microporous Mesoporous Mater.*, 2012, **160**, 10–17.
114 Z. Zhan, J. Shao, Y. Peng, Z. Wang and Y. Yan, *J. Membr. Sci.*, 2014, **471**, 299–307.
115 M. Severance, B. Wang, K. Ramasubramanian, L. Zhao, W. S. W. Ho and P. K. Dutta, *Langmuir*, 2014, **30**, 6929–6937.
116 B. Wang, C. Sun, Y. Li, L. Zhao, W. S. W. Ho and P. K. Dutta, *Microporous Mesoporous Mater.*, 2015, **208**, 72–82.
117 A. J. Brown, N. A. Brunelli, K. Eum, F. Rashidi, J. R. Johnson, W. J. Koros, C. W. Jones and S. Nair, *Science*, 2014, **345**, 72–75.
118 Y. Li, L. H. Wee, A. Volodin, J. A. Martens and I. F. J. Vankelecom, *Chem. Commun.*, 2015, **15**, 918–920.
119 F. Cacho-Bailo, S. Catalán-Aguirre, M. Etxeberría-benavides, V. Sebastian, C. Téllez and J. Coronas, *J. Membr. Sci.*, 2015, **476**, 277–285.
120 Y. Yushan, M. E. Davis and G. R. Gavalas, *J. Membr. Sci.*, 1997, **123**, 95–103.
121 A. Navajas, R. Mallada, C. Téllez, J. Coronas, M. Menéndez and J. Santamaría, *J. Membr. Sci.*, 2006, **270**, 32–41.
122 M. B. Berry, B. E. Libby, K. Rose, K. H. Haas and R. W. Thompson, *Microporous Mesoporous Mater.*, 2000, **39**, 205–217.
123 G. Li, X. H. Su and R. Sen Lin, *Mater. Lett.*, 2007, **61**, 4576–4578.
124 M. Nomura, T. Yamaguchi and S. Nakao, *Ind. Eng. Chem. Res.*, 1997, **36**, 4217–4223.
125 M. Nomura, T. Yamaguchi and S. I. Nakao, *J. Membr. Sci.*, 2001, **187**, 203–212.
126 A. I. Labropoulos, C. P. Athanasekou, N. K. Kakizis, A. A. Sapalidis, G. I. Pilatos, G. E. Romanos and N. K. Kanellopoulos, *Chem. Eng. J.*, 2014, **255**, 377–393.
127 X. Zhu, H. Wang and Y. S. Lin, *Ind. Eng. Chem. Res.*, 2010, **49**, 10026–10033.
128 M. Kanezashi and Y. S. Lin, *J. Phys. Chem. C*, 2009, **113**, 3767–3774.
129 M. Kanezashi, J. O'Brien-Abraham and Y. S. Lin, *AIChE J.*, 2008, **54**, 1478–1486.
130 Z. Tang, J. Dong and T. M. Nenoff, *Langmuir*, 2009, **25**, 4848–4852.
131 M. Tsapatsis and G. Gavalas, *J. Membr. Sci.*, 1994, **87**, 281–296.

132 W. V. Chiu, I.-S. Park, K. Shqau, J. C. White, M. C. Schillo, W. S. W. Ho, P. K. Dutta and H. Verweij, *J. Membr. Sci.*, 2011, **377**, 182–190.
133 Y. Kuwahara, T. Kamegawa, K. Mori, Y. Matsumura and H. Yamashita, *Top. Catal.*, 2009, **52**, 643–648.
134 Y. Kuwahara, K. Maki, Y. Matsumura, T. Kamegawa, K. Mori and H. Yamashita, *J. Phys. Chem. C*, 2009, **113**, 1552–1559.
135 Z. Hong, C. Zhang, X. Gu, W. Jin and N. Xu, *J. Membr. Sci.*, 2011, **366**, 427–435.
136 N. Kosinov, V. G. P. Sripathi and E. J. M. Hensen, *Microporous Mesoporous Mater.*, 2014, **194**, 24–30.
137 S. Qiu, M. Xue and G. Zhu, *Chem. Soc. Rev.*, 2014, **43**, 6116–6140.
138 R. Krishna and L. J. P. van den Broeke, *Chem. Eng. J.*, 1995, **57**, 155–162.
139 R. Krishna and J. A. Wesselingh, *Chem. Eng. Sci.*, 1997, **52**, 861–911.
140 F. Kapteijn, J. A. Moulijn and R. Krishna, *Chem. Eng. Sci.*, 2000, **55**, 2923–2930.
141 R. Krishna and R. Baur, *Sep. Purif. Technol.*, 2003, **33**, 213–254.
142 R. Krishna, *J. Phys. Chem. C*, 2009, **113**, 19756–19781.
143 R. Krishna, *Microporous Mesoporous Mater.*, 2014, **185**, 30–50.
144 A. I. Skoulidas and D. S. Sholl, *AIChE J.*, 2005, **51**, 867–877.
145 T. J. H. Vlugt, R. Krishna and B. Smit, *J. Phys. Chem. B*, 1999, **103**, 1102–1118.
146 P. F. Lito, A. S. Santiago, S. P. Cardoso, B. R. Figueiredo and C. M. Silva, *J. Membr. Sci.*, 2011, **367**, 21–32.
147 K. Y. Foo and B. H. Hameed, *Chem. Eng. J.*, 2010, **156**, 2–10.
148 R. Krishna and J. M. van Baten, *Langmuir*, 2010, **26**, 10854–10867.
149 R. Krishna and D. Paschek, *Ind. Eng. Chem. Res.*, 2000, **39**, 2618–2622.
150 A. L. Myers and J. M. Prausnitz, *AIChE J.*, 1965, **11**, 121–127.
151 R. Krishna and D. Paschek, *Sep. Purif. Technol.*, 2000, **21**, 111–136.
152 D. P. Valenzuela, A. L. Myers, O. Talu and I. Zwiebel, *AIChE J.*, 1988, **34**, 397–402.
153 L. Lu, Y. Zhu, X. Wu, S. Wang, W. Cao and X. Lu, *Sep. Sci. Technol.*, 2014, **49**, 1215–1226.
154 P. Bai, M. Tsapatsis and J. I. Siepmann, *Langmuir*, 2012, **28**, 15566–15576.
155 E. Costa, J. L. Sotelo, G. Calleja and C. Marron, *AIChE J.*, 1981, **27**, 5–12.
156 E. Costa, G. Calleja, C. Marron, A. Jimenez and J. Pau, *J. Chem. Eng. Data*, 1989, **34**, 156–160.
157 S. Sochard, N. Fernandes and J. Reneaume, *AIChE J.*, 2010, **56**, 3109–3119.
158 A. Erto, A. Lancia and D. Musmarra, *Microporous Mesoporous Mater.*, 2012, **154**, 45–50.
159 M. Mofarahi and F. Gholipour, *Microporous Mesoporous Mater.*, 2014, **200**, 1–10.
160 A. I. Skoulidas, D. S. Sholl and R. Krishna, *Langmuir*, 2003, **19**, 7977–7988.
161 R. Krishna, J. M. Van Baten, E. Garcia-Perez and S. Calero, *Ind. Eng. Chem. Res.*, 2007, **46**, 2974–2986.
162 R. Krishna and J. M. Van Baten, *Microporous Mesoporous Mater.*, 2008, **109**, 91–108.
163 R. Krishna and J. M. Van Baten, *Chem. Phys. Lett.*, 2006, **420**, 545–549.
164 C. Chmelik, L. Heinke, J. Kärger, W. Schmidt, D. B. Shah, J. M. Van Baten and R. Krishna, *Chem. Phys. Lett.*, 2008, **459**, 141–145.
165 R. Krishna and J. M. van Baten, *Phys. Chem. Chem. Phys.*, 2013, **15**, 7994–8016.
166 D. Paschek and R. Krishna, *Langmuir*, 2001, **17**, 247–254.
167 F. van Kapteijn, J. A. Moulijn, J. M. de Graaf and J. ChE, *AIChE J.*, 1999, **45**, 497–511.
168 R. Krishna and J. M. van Baten, *J. Membr. Sci.*, 2011, **383**, 289–300.
169 R. Krishna and J. M. Van Baten, *Chem. Eng. Sci.*, 2009, **64**, 3159–3178.
170 L. J. P. Van den Broeke and R. Krishna, *Chem. Eng. Sci.*, 1995, **50**, 2507–2522.
171 R. Krishna, *Chem. Phys. Lett.*, 2000, **326**, 477–484.
172 R. Krishna and D. Paschek, *Chem. Eng. J.*, 2002, **87**, 1–9.
173 D. M. Ruthven, M. Eic and E. Richard, *Zeolites*, 1991, **11**, 647–653.
174 S. Brandani, M. Jama and D. Ruthven, *Microporous Mesoporous Mater.*, 2000, **35–36**, 283–300.
175 D. M. Ruthven, *Adsorption*, 2007, **13**, 225–230.
176 G. Xomeritakis, S. Nair and M. Tsapatsis, *Microporous Mesoporous Mater.*, 2000, **38**, 61–73.
177 J. B. Lee, H. H. Funke, R. D. Noble and J. L. Falconer, *J. Membr. Sci.*, 2009, **341**, 238–245.
178 R. Krishna and J. Baten, *Chem. Eng. J.*, 2008, **140**, 614–620.
179 W. Zhu, P. Hrabanek, L. Gora, F. Kapteijn, J. C. Jansen, J. A. Moulijn and B. Part, *Stud. Surf. Sci. Catal.*, 2004, **154**, 1935–1943.
180 R. Krishna and J. M. van Baten, *Langmuir*, 2010, **26**, 8450–8463.
181 R. Krishna and J. M. van Baten, *J. Membr. Sci.*, 2010, **360**, 476–482.
182 T. C. Bowen, J. C. Wyss, R. D. Noble and J. L. Falconer, *Ind. Eng. Chem. Res.*, 2004, **43**, 2598–2601.
183 R. Krishna and J. M. van Baten, *J. Phys. Chem. C*, 2010, **114**, 13154–13156.
184 K. Zhang, R. P. Lively, M. E. Dose, L. Li, W. J. Koros, D. M. Ruthven, B. A. McCool and R. R. Chance, *Microporous Mesoporous Mater.*, 2013, **170**, 259–265.
185 K. Zhang, R. P. Lively, C. Zhang, W. J. Koros and R. R. Chance, *J. Phys. Chem.*, 2013, **117**, 7214–7225.
186 K. Zhang, R. P. Lively, M. E. Dose, A. J. Brown, C. Zhang, J. Chung, S. Nair, W. J. Koros and R. R. Chance, *Chem. Commun.*, 2013, **49**, 3245–3247.
187 F. Kapteijn, W. J. W. Bakker, J. Van De Graaf, G. Zheng, J. Poppe and J. A. Moulijn, *Catal. Today*, 1995, **25**, 213–218.
188 T. Wu, M. C. Diaz, Y. Zheng, R. Zhou, H. H. Funke, J. L. Falconer and R. D. Noble, *J. Membr. Sci.*, 2015, **473**, 201–209.

189 T. Q. Gardner, J. L. Falconer and R. D. Noble, *AIChE J.*, 2004, **50**, 2816–2834.
190 J. Shao, Z. Zhan, J. Li, Z. Wang, K. Li and Y. Yan, *J. Membr. Sci.*, 2014, **451**, 10–17.
191 H. Zhou, D. Korelskiy, T. Leppäjärvi, M. Grahn, J. Tanskanen and J. Hedlund, *J. Membr. Sci.*, 2012, **399–400**, 106–111.
192 M. Grahn and J. Hedlund, *J. Membr. Sci.*, 2014, **471**, 328–337.
193 S. Farooq and I. Karimi, *J. Membr. Sci.*, 2001, **186**, 109–121.
194 J. G. Martinek, T. Q. Gardner, R. D. Noble and J. L. Falconer, *Ind. Eng. Chem. Res.*, 2006, **45**, 6032–6043.
195 H. Li, U. Schygulla, J. Hoffmann, P. Niehoff, K. Haas-Santo and R. Dittmeyer, *Chem. Eng. Sci.*, 2014, **108**, 94–102.
196 J. M. van de Graaf, E. van der Bijl, A. Stol, F. Kapteijn and J. A. Moulijn, *Ind. Eng. Chem. Res.*, 1998, **37**, 4071–4083.
197 J. M. van de Graaf, F. Kapteijn and J. A. Moulijn, *J. Membr. Sci.*, 1998, **144**, 87–104.
198 T. C. Bowen, R. D. Noble and J. L. Falconer, *J. Membr. Sci.*, 2004, **245**, 1–33.
199 S. Bhattacharya and S. Hwang, *J. Membr. Sci.*, 1997, **132**, 73–90.
200 A. M. Avila, H. H. Funke, Y. Zhang, J. L. Falconer and R. D. Noble, *J. Membr. Sci.*, 2009, **335**, 32–36.
201 G. He, Y. Mi, P. L. Yue and G. Chen, *J. Membr. Sci.*, 1999, **153**, 243–258.
202 B. Raghunath and S. Hwang, *J. Membr. Sci.*, 1992, **65**, 147–161.
203 G. Ji, G. Wang, K. Hooman, S. Bhatia and J. C. D. da Costa, *Chem. Eng. J.*, 2013, **218**, 394–404.
204 G. Ji, G. Wang, K. Hooman, S. Bhatia and J. C. D. da Costa, *Chem. Eng. Sci.*, 2014, **111**, 142–152.
205 E. Kim, J. Choi and M. Tsapatsis, *Microporous Mesoporous Mater.*, 2013, **170**, 1–8.
206 J. Hedlund, D. Korelskiy, L. Sandström and J. Lindmark, *J. Membr. Sci.*, 2009, **345**, 276–287.
207 M. Yu, R. D. Noble and J. L. Falconer, *Acc. Chem. Res.*, 2011, **44**, 1196–1206.
208 E. E. Mallon, M. Y. Jeon, M. Navarro, A. Bhan and M. Tsapatsis, *Langmuir*, 2013, **29**, 6546–6555.
209 M. E. Dose, K. Zhang, J. A. Thompson, J. Leisen, R. R. Chance and W. J. Koros, *Chem. Mater.*, 2014, **26**, 4368–4376.
210 P. H. Nelson, M. Tsapatsis and S. M. Auerbach, *J. Membr. Sci.*, 2001, **184**, 245–255.
211 J. Kangas, L. Sandström, I. Malinen, J. Hedlund and J. Tanskanen, *J. Membr. Sci.*, 2013, **435**, 186–206.
212 W. Ding, H. Li, P. Pfeifer and R. Dittmeyer, *Chem. Eng. J.*, 2014, **254**, 545–558.
213 Y. J. Colón and R. Q. Snurr, *Chem. Soc. Rev.*, 2014, **43**, 5735–5749.
214 E. Haldoupis, S. Nair and D. S. Sholl, *Phys. Chem. Chem. Phys.*, 2011, **13**, 5053–5060.
215 E. L. First, C. E. Gounaris, J. Wei and C. a. Floudas, *Phys. Chem. Chem. Phys.*, 2011, **13**, 17339–17358.
216 E. L. First, C. E. Gounaris and C. A. Floudas, *Langmuir*, 2013, **29**, 5599–5608.
217 E. L. First and C. A. Floudas, *Microporous Mesoporous Mater.*, 2013, **165**, 32–39.
218 R. L. Martin, T. F. Willems, L.-C. Lin, J. Kim, J. a. Swisher, B. Smit and M. Haranczyk, *ChemPhysChem*, 2012, **13**, 3595–3597.
219 J. Kim, L.-C. Lin, R. L. Martin, J. A. Swisher, M. Haranczyk and B. Smit, *Langmuir*, 2012, **28**, 11914–11919.
220 J. Kim, M. Abouelnasr, L.-C. Lin and B. Smit, *J. Am. Chem. Soc.*, 2013, **135**, 7545–7552.
221 E. L. First, M. M. F. Hasan and C. A. Floudas, *AIChE J.*, 2014, **60**, 1767–1785.
222 P. Bai, M. Y. Jeon, L. Ren, C. Knight, M. W. Deem, M. Tsapatsis and J. I. Siepmann, *Nat. Commun.*, 2015, **6**, 5912.
223 H. Voss, A. Diefenbacher, G. Schuch, H. Richter, I. Voigt, M. Noack and J. Caro, *J. Membr. Sci.*, 2009, **329**, 11–17.
224 S. Li, J. L. Falconer and R. D. Noble, *Adv. Mater.*, 2006, **18**, 2601–2603.
225 S. Li, M. A. Carreon, Y. Zhang, H. H. Funke, R. D. Noble and J. L. Falconer, *J. Membr. Sci.*, 2010, **352**, 7–13.
226 J. van den Bergh, W. Zhu, J. Gascon, J. A. Moulijn and F. Kapteijn, *J. Membr. Sci.*, 2008, **316**, 35–45.
227 M. Simo, in *Separation and purification technologies in biorefineries*, ed. S. Ramaswamy, H.-J. Huang and B. V. Ramarao, John Wiley & Sons, UK, 2013.
228 J. S. Jeong, H. Jeon, K. M. Ko, B. Chung and G. W. Choi, *Renewable Energy*, 2012, **42**, 41–45.
229 L. Y. Jiang, Y. Wang, T. S. Chung, X. Y. Qiao and J. Y. Lai, *Prog. Polym. Sci.*, 2009, **34**, 1135–1160.
230 N. Le and T. S. Chung, *J. Membr. Sci.*, 2014, **454**, 62–73.
231 K. Vanherck, G. Koecklberghs and I. F. J. Vankelecom, *Prog. Polym. Sci.*, 2013, **38**, 874–896.
232 Y. Xu, C. Chen and J. Li, *Chem. Eng. Sci.*, 2007, **62**, 2466–2473.
233 Y. Morigami, M. Kondo, J. Abe, H. Kita and K. Okamoto, *Sep. Purif. Technol.*, 2001, **25**, 251–260.
234 K. Sato, K. Aoki, K. Sugimoto, K. Izumi, S. Inoue, J. Saito, S. Ikeda and T. Nakane, *Microporous Mesoporous Mater.*, 2008, **115**, 184–188.
235 K. Sato and T. Nakane, *J. Membr. Sci.*, 2007, **301**, 151–161.
236 H. Richter, I. Voigt and J.-T. Kuehnert, *Desalination*, 2006, **199**, 92–93.
237 T. Gallego-Lizón, E. Edwards, G. Lobiundo and L. F. Santos, *J. Membr. Sci.*, 2002, **197**, 309–319.
238 A. Urtiaga, E. D. Gorri, C. Casado and I. Ortiz, *Sep. Purif. Technol.*, 2003, **32**, 207–213.
239 Y. S. Li and W. S. Yang, *Chin. J. Catal.*, 2015, **36**, 692–697.
240 X. Wang, Y. Chen, C. Zhang, X. Gu and N. Xu, *J. Membr. Sci.*, 2014, **455**, 294–304.
241 X. Wang, Z. Yang, C. Yu, L. Yin, C. Zhang and X. Gu, *Microporous Mesoporous Mater.*, 2014, **197**, 17–25.
242 Y. Liu, Z. Yang, C. Yu, X. Gu and N. Xu, *Microporous Mesoporous Mater.*, 2011, **143**, 348–356.
243 X. Gu, Nanjing University of Technology and Jiangsu Nine Heaven High-Tech Co. Ltd., personal information.
244 Y. S. Li and W. S. Yang, Dalian Institute of Chemical Physics, Chinese Academy of Sciences, personal information.

245 Y. S. Li, H. L. Chen, J. Liu and W. S. Yang, *J. Membr. Sci.*, 2006, **277**, 230–239.
246 H. Zhou, Y. S. Li, G. Q. Zhu, J. Liu and W. S. Yang, *Sep. Purif. Technol.*, 2009, **65**, 164–172.
247 Y. S. Li, J. Liu and W. S. Yang, *J. Membr. Sci.*, 2006, **281**, 646–657.
248 Y. S. Li and W. S. Yang, *J. Membr. Sci.*, 2008, **316**, 3–17.
249 G. Q. Zhu, Y. S. Li, H. L. Chen and W. S. Yang, *J. Mater. Sci.*, 2008, **43**, 3279–3288.
250 Y. S. Li, H. L. Chen and W. S. Yang, *Chin. J. Catal.*, 2006, **27**, 544–549.
251 C. Téllez and M. Menéndez, in *Membranes for Membrane Reactors: Preparation, Optimization and Selection*, ed. A. Basile and F. Gallucci, John Wiley & Sons, UK, 2011.
252 M. O. Daramola, E. F. Aransiola and T. V. Ojumu, *Materials*, 2012, **5**, 2101–2136.
253 *Chemical Engineering and Processing: Process Intensification*, 2015, vol. 88, pp. 1–98.
254 E. Drioli and E. Fontanova, *Ullmann's Encyclopaedia of Industrial Chemistry*, Wiley-VCH, Weinheim, 2010.
255 E. Fontanova and E. Drioli, *Chem. Ing. Tech.*, 2014, **86**, 2039–2050.
256 R. Dittmeyer and J. Caro, in *Handbook of Heterogeneous Catalysis*, ed. G. Ertl, H. Knözinger, F. Schüth and J. Weitkamp, Wiley-VCH, pp. 2198–2247.
257 J. Caro, in *Comprehensive Membrane Science and Technology*, ed. E. Drioli and L. Giorno, Elsevier, 2010, pp. 1–24.
258 S. Khajavi, S. Sartipi, J. Gascon, J. C. Jansen and F. Kapteijn, *Microporous Mesoporous Mater.*, 2010, **132**, 510–517.
259 S. Khajavi, F. Kapteijn and J. C. Jansen, *J. Membr. Sci.*, 2007, **299**, 63–72.
260 S.-R. Lee, Y.-H. Son, A. Julbe and J.-H. Choy, *Thin Solid Films*, 2006, **495**, 92–96.
261 A. Julbe, J. Motuzas, F. Cazeville, G. Volle and C. Guizard, *Sep. Purif. Technol.*, 2003, **32**, 139–149.
262 N. Wang, Y. Liu, A. Huang and J. Caro, *Microporous Mesoporous Mater.*, 2015, **207**, 33–38.
263 C. Günther, H. Richter and I. Voigt, *Chem. Eng. Trans.*, 2013, **32**, 1963–1968.
264 S.-J. Kim, S. Yang, G. K. Reddy, P. Smirniotis and J. Dong, *Energy Fuels*, 2013, **27**, 4471–4480.
265 Y. Zhang, Z. Wu, Z. Hong, X. Gu and N. Xu, *Chem. Eng. J.*, 2012, **197**, 314–321.
266 S. M. Maier, A. Jentys and J. A. Lercher, *J. Phys. Chem. C*, 2011, **115**, 8005–8013.
267 H. K. Beyer, *Molecular Sieves: Science and Technology, Post-Synthesis Modification I*, Springer Berlin Heidelberg, 2002.
268 G. Kennedy, S. Lawton, A. Fung, M. Rubin and S. Steuernagel, *Catal. Today*, 1999, **49**, 385–399.
269 G. Kennedy, S. Lawton and M. Rubin, *J. Am. Chem. Soc.*, 1994, **116**, 11000–11003.
270 D. Ma, F. Deng, R. Fu, X. Dan and X. Bao, *J. Phys. Chem. B*, 2001, **105**, 1770–1779.
271 R. Kreiter, M. Rietkerk, H. Castricum, H. van Veen, J. ten Elshof and J. Vente, *J. Sol-Gel Sci. Technol.*, 2011, **57**, 245–252.
272 B. Elyassi, X. Zhang and M. Tsapatsis, *Microporous Mesoporous Mater.*, 2014, **193**, 134–144.
273 K. Sato, K. Sugimoto, Y. Sekine, M. Takada, M. Matsukata and T. Nakane, *Microporous Mesoporous Mater.*, 2007, **101**, 312–318.
274 K.-I. Sawamura, T. Shirai, M. Takada, Y. Sekine, E. Kikuchi and M. Matsukata, *Catal. Today*, 2008, **132**, 182–187.
275 S. A. S. Rezai, J. Lindmark, C. Andersson, F. Jareman, K. Moller and J. Hedlund, *Microporous Mesoporous Mater.*, 2008, **108**, 136–142.
276 T. Masuda, N. Fukumoto and M. Kitamura, *Microporous Mesoporous Mater.*, 2001, **48**, 239–245.
277 S. J. Kim, Z. Xu, G. K. Reddy, P. Smirniotis and J. H. Dong, *Ind. Eng. Chem. Res.*, 2012, **51**, 1364–1375.
278 M. P. Bernal, E. Piera, J. Coronas, M. Menéndez and J. Santamarıa, *Catal. Today*, 2000, **56**, 221–227.
279 H. Wang and Y. S. Lin, *AIChE J.*, 2012, **58**, 153–162.
280 J. Canivet, A. Fateeva, Y. Guo, B. Coasne and D. Farusseng, *Chem. Soc. Rev.*, 2014, **43**, 5594–5617.
281 N. C. Burtch, H. Jasuja and K. S. Walton, *Chem. Rev.*, 2014, **114**, 10575–10612.
282 J. J. Low, A. I. Benin, P. Jakubczak, J. F. Abrahamian, S. A. Faheem and R. R. Willis, *J. Am. Chem. Soc.*, 2009, **131**, 15834–15842.
283 A. Huang, W. Dou and J. Caro, *J. Am. Chem. Soc.*, 2010, **132**, 15562–15564.
284 A. Huang, Y. Chen, Q. Liu, N. Wang, J. Jiang and J. Caro, *J. Membr. Sci.*, 2014, **454**, 126–132.
285 J. Caro, *Curr. Opin. Chem. Eng.*, 2011, **1**, 77–83.
286 S. R. Batten, N. R. Champness, X.-M. Chen, J. Garcia-Martinez, S. Kitagawa, L. Öhrström, M. O'Keffe, M. P. Suh and J. Reedijk, *CrystEngComm*, 2012, **14**, 3001–3004.
287 C. A. Fyfe, G. Kokotailo, G. Kennedy and C. de Schutter, *J. Chem. Soc., Chem. Commun.*, 1985, 306–308.
288 C. A. Fyfe, G. J. Kennedy, G. T. Kokotailo, J. R. Lyerla and W. W. Fleming, *J. Chem. Soc., Chem. Commun.*, 1985, 740–742.
289 W. C. Conner, R. Vincent, P. Man and J. Fraissard, *Catal. Lett.*, 1990, **4**, 75–84.
290 C. Cui, Y. Liu, H. Xu, S. Li, W. Zhang, P. Cui and F. Huo, *Small*, 2014, **10**, 3672–3676.
291 G. Lu, C. Cui, W. Zhang, Y. Liu and F. Huo, *Chem. – Asian J.*, 2013, **8**, 69–72.
292 M. E. Silvestre, M. Franzreb, P. G. Weidler, O. Shekhah and C. Woll, *Adv. Funct. Mater.*, 2013, **23**, 1210–1213.
293 M. C. So, S. Jin, H.-J. Son, G. P. Wiederrecht, O. K. Farha and J. T. Hupp, *J. Am. Chem. Soc.*, 2013, **135**, 15698–15701.
294 D. Witters, S. Vermeir, R. Puers, B. F. Sels, D. E. De Vos, J. Lammertyn and R. Ameloot, *Chem. Mater.*, 2013, **25**, 1021–1023.
295 J. T. Joyce, F. R. Laffir and C. Silien, *J. Phys. Chem. C*, 2013, **117**, 12502–12509.
296 D. Y. Lee, E.-K. Kim, C. Y. Shin, D. V. Shinde, W. Lee, N. K. Shrestha, J. K. Lee and S.-H. Han, *RSC Adv.*, 2014, **4**, 12037–12042.
297 G. Xu, T. Yamada, K. Otsubo, S. Sakaida and H. Kitagawa, *J. Am. Chem. Soc.*, 2012, **134**, 16524–16527.

298 M. Li and M. Dinca, *Chem. Sci.*, 2014, **5**, 107–111.
299 I. Hod, W. Bury, D. M. Karlin, P. Deria, C.-W. Kung, M. J. Katz, M. So, B. Klahr, D. Jin, Y.-W. Chung, T. W. Odom, O. K. Farha and J. T. Hupp, *Adv. Mater.*, 2014, **26**, 6295–6300.
300 N. Campagnol, E. R. Souza, D. E. De Vos, K. Binnemans and J. Fransaer, *Chem. Commun.*, 2014, **50**, 12545–12547.
301 N. Campagnol, T. Van Assche, T. Boudewijns, J. Denayer, K. Binnemans, D. De Vos and J. Fransaer, *J. Mater. Chem. A*, 2013, **1**, 5827–5830.
302 W. Liang and D. M. D'Alessandro, *Chem. Commun.*, 2013, **49**, 3706–3708.
303 Z.-Q. Li, M. Zhang, B. Liu, C.-Y. Guo and M. Zhou, *Inorg. Chem. Commun.*, 2013, **36**, 241–244.
304 J. Yao, D. Dong, D. Li, L. He, G. Xu and H. Wang, *Chem. Commun.*, 2011, **47**, 2559–2561.
305 A. J. Brown, J. R. Johnson, M. E. Lydon, W. J. Koros, C. W. Jones and S. Nair, *Angew. Chem., Int. Ed. Engl.*, 2012, **124**, 10767–10770.
306 H. T. Kwon and H.-K. Jeong, *J. Am. Chem. Soc.*, 2013, **135**, 10763–10768.
307 D. Zacher, O. Shekhah, C. Wöll and R. A. Fischer, *Chem. Soc. Rev.*, 2009, **38**, 1418–1429.
308 Z. Lai, G. Bonilla, I. Diaz, J. G. Nery, K. Sujaoti, M. A. Amat, E. Kokkoli, O. Terasaki, R. W. Thompson, M. Tsapatsis and D. G. Vlachos, *Science*, 2003, **300**, 456–460.
309 M. W. Deem, R. Pophale, P. A. Cheeseman and D. J. Earl, *J. Phys. Chem.*, 2009, **113**, 21353–21360.
310 Z. Kang, M. Xue, L. Fan, J. Ding, L. Guo, L. Gao and S. Qiu, *Chem. Commun.*, 2013, **49**, 10569–10571.
311 D. Nagaraju, D. G. Bhagat, R. Banerjee and U. K. Kharul, *J. Mater. Chem. A*, 2013, **1**, 8828–8835.
312 A. Huang, Y. Chen, N. Wang, Z. Hu, J. Jiang and J. Caro, *Chem. Commun.*, 2012, **48**, 10981–10983.
313 S. Fan, F. Sun, J. Xie, J. Guo, L. Zhang, C. Wang, Q. Pan and G. Zhu, *J. Mater. Chem. A*, 2013, **1**, 11438–11442.
314 T. Ben, C. Lu, C. Pei, S. Xu and S. Qiu, *Chem. – Eur. J.*, 2012, **18**, 10250–10253.
315 F. Zhang, X. Zou, X. Gao, S. Fan, F. Sun, H. Ren and G. Zhu, *Adv. Funct. Mater.*, 2012, **22**, 3583–3590.
316 K. Huang, S. Liu, Q. Li and W. Jin, *Sep. Purif. Technol.*, 2013, **119**, 94–101.
317 X. Dong, K. Huang, S. Liu, R. Ren, W. Jin and Y. S. Lin, *J. Mater. Chem.*, 2012, **22**, 19222–19227.
318 X. Dong and Y. S. Lin, *Chem. Commun.*, 2013, **49**, 1196–1198.
319 O. M. Yaghi, M. O'Keeffe, N. W. Ockwick, H. K. Chae, M. Eddaoudi and J. Kim, *Nature*, 2003, **423**, 705–714.
320 M. Eddaoudi, J. Kim, N. Rosi, D. Vodak, J. Wachter, M. O'Keeffe and O. M. Yaghi, *Science*, 2002, **295**, 469–472.
321 R. Banerjee, H. Furukawa, D. Britt, C. Knobler, M. O'Keeffe and O. M. Yaghi, *J. Am. Chem. Soc.*, 2009, **131**, 3875–3877.
322 S. P. Kyo, Z. Ni, A. P. Cote, J. Y. Choi, R. Huang, F. J. Uribe-Romo, H. K. Chae, M. O'Keeffe and O. M. Yaghi, *Proc. Natl. Acad. Sci. U. S. A.*, 2006, **103**, 10186–10191.
323 S. Tanaka, T. Shimada, K. Fujita, Y. Miyake, K. Kida, K. Yogo, J. F. M. Denayer, M. Sugita and T. Takewaki, *J. Membr. Sci.*, 2014, **472**, 29–38.
324 Y. Pan, T. Li, G. Lestari and Z. Lai, *J. Membr. Sci.*, 2012, **390–391**, 93–98.
325 H. T. Kwon and H.-K. Jeong, *Chem. Eng. Sci.*, 2015, **124**, 20–26.
326 Y. Pan and Z. Lai, *Chem. Commun.*, 2011, **47**, 10275–10277.
327 L. Diestel, H. Bux, D. Wachsmuth and J. Caro, *Microporous Mesoporous Mater.*, 2012, **164**, 288–293.
328 K. Zhang, R. P. Lively, C. Zhang, R. R. Chance, W. J. Koros, D. S. Sholl and S. Nair, *J. Phys. Chem. Lett.*, 2013, **4**, 3618–3622.
329 C. Gücüyener, J. van den Bergh, J. Gascon and F. Kapteijn, *J. Am. Chem. Soc.*, 2010, **132**, 17704–17706.
330 D. Fairen-Jimenez, S. A. Moggach, M. T. Wharmby, P. A. Wright, S. Parsons and T. Düren, *J. Am. Chem. Soc.*, 2001, **133**, 8900–8902.
331 S. A. Moggach, T. D. Bennett and A. K. Cheetham, *Angew. Chem.*, 2009, **121**, 7221–7223.
332 T. Chokbunpiam, R. Chanajaree, T. Remsungnen, O. Saengsawang, S. Fritzsche, C. Chmelik, J. Caro, W. Janke and S. Hannongbua, *Microporous Mesoporous Mater.*, 2014, **187**, 1–6.
333 S. Aguado, G. Bergeret, M. P. Titus, V. Moizan, C. Nieto-Draghi, N. Bats and D. Farrusseng, *New J. Chem.*, 2011, **35**, 546–550.
334 J. van den Bergh, C. Gücüyener, E. A. Pidko, E. J. M. Hensen, J. Gascon and F. Kapteijn, *Chem. – Eur. J.*, 2011, **17**, 8832–8840.
335 D. L. Chen, N. Wang, F. F. Wang, J. Xie, Y. Zhong, W. Zhu, J. K. Johnson and R. Krishna, *J. Phys. Chem. C*, 2014, **118**, 17831–17837.
336 C. O. Ania, E. García-Pérez, M. Haro, J. J. Gutiérrez-Sevillano, T. Valdés-Solís, J. B. Parra and S. Calero, *J. Phys. Chem. Lett.*, 2012, **3**, 1159–1164.
337 H. Bux, F. Liang, Y. Li, J. Cravillon, M. Wiebcke and J. Caro, *J. Am. Chem. Soc.*, 2009, **131**, 16000–16001.
338 M. R. Ryder, B. Civalleri, T. D. Bennett, S. Henke, S. Rudic, G. Cinque, F. F. Alonso and J. C. Tan, *Phys. Rev. Lett.*, 2014, **113**, 215502.
339 J. A. Thompson, C. R. Blad, N. A. Brunelli, M. E. Lydon, R. P. Lively, C. W. Jones and S. Nair, *Chem. Mater.*, 2012, **14**, 1930–1936.
340 K. Eum, K. C. Jayachandrababu, F. Rashidi, K. Zhang, J. Leisen, S. Graham, R. P. Lively, R. R. Chance, D. S. Sholl, C. W. Jones and S. Nair, *J. Am. Chem. Soc.*, 2015, **137**, 4191–4197.
341 T. Li, Y. Pan, K.-V. Peinemann and Z. Lai, *J. Membr. Sci.*, 2013, **425–426**, 235–242.
342 B. Zornoza, A. Martinez-Joaristi, P. Serra-Crespo, C. Tellez, J. Coronas, J. Gascon and F. Kapteijn, *Chem. Commun.*, 2011, **47**, 9522–9524.
343 X. L. Liu, Y. S. Li, G. Q. Zhu, Y. J. Ban, L. Y. Xu and W. S. Yang, *Angew. Chem., Int. Ed.*, 2011, **50**, 10636–10639.
344 T. Yang, Y. Xiao and T.-S. Chung, *Energy Environ. Sci.*, 2011, **4**, 4171.
345 T. Rodenas, M. Van Dalen, E. García-Pérez, P. Serra-Crespo, B. Zornoza, F. Kapteijn and J. Gascon, *Adv. Funct. Mater.*, 2014, **24**, 249–256.

346 H. B. T. Jeazet, C. Staudt and C. Janiak, *Chem. Commun.*, 2012, **48**, 2140–2142.
347 B. Seoane, V. Sebastian, C. Tellez and J. Coronas, *CrystEngComm*, 2013, **15**, 9483–9490.
348 M. Valero, B. Zornoza, C. Tellez and J. Coronas, *Microporous Mesoporous Mater.*, 2014, **192**, 23–28.
349 J. A. Thompson, J. T. Vaughn, N. A. Brunelli, W. J. Koros, C. W. Jones and S. Nair, *Microporous Mesoporous Mater.*, 2014, **192**, 43–51.
350 X. Guo, H. Huang, Y. Ban, Q. Yang, Y. Xiao, Y. Li, W. Yang and C. Zhong, *J. Membr. Sci.*, 2015, **478**, 130–139.
351 X. Y. Chen, V. T. Hoang, D. Rodrigue and S. Kaliaguine, *RSC Adv.*, 2013, **3**, 24266–24279.
352 C. J. Duan, G. D. Kang, D. D. Liu, L. N. Wang, C. Jiang, Y. M. Cao and Q. Yuan, *J. Appl. Polym. Sci.*, 2014, **131**, 40719.
353 D. S. Zhang, Z. Chang, Y. F. Li, Z. Y. Jiang, Z. H. Xuan, Y. H. Zhang, J. R. Li, Q. Chen, T. L. Hu and X. H. Bu, *Sci. Rep.*, 2013, **3**, 3312.
354 F. Dorosti, M. Omidkhah and R. Abedini, *Chem. Eng. Res. Des.*, 2014, **92**, 2439–2448.
355 S. Shahid and K. Nijmeijer, *J. Membr. Sci.*, 2014, **459**, 33–44.
356 J. O. Hsieh, K. J. Balkus, J. P. Ferraris and I. H. Musselman, *Microporous Mesoporous Mater.*, 2014, **196**, 165–174.
357 S. Shahid and K. Nijmeijer, *J. Membr. Sci.*, 2014, **470**, 166–177.
358 T. X. Yang and T. S. Chung, *J. Mater. Chem. A*, 2013, **1**, 6081–6090.
359 T. H. Bae and J. R. Long, *Energy Environ. Sci.*, 2013, **6**, 3565–3569.
360 R. Abedini, M. Omidkhah and F. Dorosti, *Int. J. Hydrogen Energy*, 2014, **39**, 7897–7909.
361 N. Nordin, A. Ismail and A. Mustafa, *J. Teknol.*, 2014, **69**, 73–76.
362 S. Basu, A. Cano-Odena and I. F. J. Vankelecom, *J. Membr. Sci.*, 2010, **362**, 478–487.
363 H. Ren, J. Jin, J. Hu and H. Liu, *Ind. Eng. Chem. Res.*, 2012, **51**, 10156–10164.
364 S. Sorribas, P. Gorgojo, C. Tellez, J. Coronas and A. G. Livingston, *J. Am. Chem. Soc.*, 2013, **135**, 15201–15208.
365 R. Lin, L. Ge, L. Hou, E. Strounina, V. Rudolph and Z. Zhu, *ACS Appl. Mater. Interfaces*, 2014, **6**, 5609–5618.
366 H.-K. Jeong, S. Nair, T. Vogt, L. C. Dickinson and M. Tsapatsis, *Nat. Mater.*, 2002, **2**, 53–58.
367 S. Choi, J. Coronas, E. Jordan, W. Oh, S. Nair, F. Onorato, D. F. Shantz and M. Tsapatsis, *Angew. Chem., Int. Ed.*, 2008, **47**, 552–555.
368 J. Choi and M. Tsapatsis, *J. Am. Chem. Soc.*, 2010, **132**, 448–449.
369 H. W. Kim, H. W. Yoon, S.-M. Yoon, B. M. Yoo, B. K. Ahn, Y. H. Cho, H. J. Shin, H. Yang, U. Paik, S. Kwon, J.-Y. Choi and H. B. Park, *Science*, 2013, **342**, 91–95.
370 J. A. Sheffel and M. Tsapatsis, *J. Membr. Sci.*, 2007, **295**, 50–70.
371 J. A. Sheffel and M. Tsapatsis, *J. Membr. Sci.*, 2009, **326**, 595–607.
372 L. Diestel, N. Wang, A. Schulz, F. Steinbach and J. Caro, *Ind. Eng. Chem. Res.*, 2015, **54**, 1103–1112.
373 H.-K. Jeong, W. Krych, H. Ramanan, S. Nair, E. Marand and M. Tsapatsis, *Chem. Mater.*, 2004, **16**, 3838–3845.

